

1 **Validation of SNPP OMPS limb profiler version 2.6 ozone profile**  
2 **retrievals against correlative satellite and ground based**  
3 **measurements**

4  
5 Nigel A. D. Richards<sup>1,2</sup>, Natalya A. Kramarova<sup>2</sup>, Stacey M. Frith<sup>3,2</sup>, Sean M. Davis<sup>4</sup> and Yue Jia<sup>5</sup>  
6

7 <sup>1</sup>Goddard Earth Sciences Technology and Research (GESTAR II), University of Maryland Baltimore County  
8 (UMBC), Baltimore, MD, USA

9 <sup>2</sup>NASA Goddard Space Flight Center, Greenbelt, MD, USA

10 <sup>3</sup>Science Systems and Applications, Inc., Lanham, MD, USA

11 <sup>4</sup>NOAA Chemical Sciences Laboratory, Boulder, CO, USA

12 <sup>5</sup>University of Texas at Dallas, Dallas, TX, USA

13  
14 *Correspondence to:* nigel.richards@nasa.gov

15

16 **Abstract.** The Ozone Mapping and Profiler Suite Limb Profiler (OMPS LP) was launched onboard the Suomi National  
17 Polar-orbiting Partnership (SNPP) satellite in 2011 and began routine science operations in April 2012. The OMPS  
18 LP uses measurements of scattered solar radiation in the ultraviolet, visible and near infrared wavelengths to retrieve  
19 high vertical resolution profiles of ozone from 12 km (or cloud tops) up to 57 km. In mid-2023, version 2.6 of the  
20 OMPS LP ozone profile retrievals was released, featuring improvements in calibration, retrieval algorithm, and data  
21 quality. We evaluate OMPS LP version 2.6 ozone retrievals using correlative data from other satellite instruments and  
22 ground based data for the period April 2012 to April 2024. Our results show agreement between OMPS LP and all  
23 correlative data sources between 20 and 50 km at all latitudes with differences of less than 10%, with OMPS generally  
24 exhibiting a negative bias, except between 32 and 38 km in the tropics and southern mid-latitudes, where the bias is  
25 positive. In the tropics and southern mid-latitudes the differences between OMPS LP and MLS, and OMPS LP and  
26 SAGE III/ISS are less than  $\pm 5\%$  between 20 and 45 km. Above 50 km, the agreement with MLS is still on the order  
27 of -5% or better. Larger positive biases, up to  $\sim 35\%$ , are seen in the upper troposphere lower stratosphere layer ( $\sim 15$   
28 to 20 km) between approximately 40° South and 40° North. We find that OMPS version 2.6 ozone exhibits the same  
29 seasonal cycle as compared to all correlative measurement sources and our analysis shows that there is no significant  
30 seasonal bias in OMPS LP. We find drifts relative to correlative observations at all latitude bands of less than  
31  $\pm 2\%$ /decade ( $\pm 1\%$ /decade) between 25 and 50 km for the 2012-2024 period, with larger drifts above 50 km and below  
32 20 km. These drifts vary between correlative measurements and straddle the zero line, we therefore conclude that there  
33 is no significant systematic drift in OMPS LP version 2.6 ozone for the period 2012 to 2024. The drift results represent  
34 an improvement in the long term stability of version 2.6 ozone over that of version 2.5.

35 **1. Introduction**

36 Stratospheric ozone is crucial for life on Earth as it acts as a protective layer absorbing harmful UV radiation. In 1985,  
37 the discovery of the Antarctic ozone hole (Farman et al., 1985) caused global public safety concerns, ultimately leading  
38 to the establishment of the Montreal Protocol in 1987. The regulations imposed by the Montreal Protocol have led to  
39 a slow recovery in upper stratospheric ozone over the 2000-2020 period. Measurements show a positive trend in upper  
40 stratospheric ozone in the range of 1.5-2.2% decade<sup>-1</sup> outside of the polar regions at mid-latitudes in both hemispheres  
41 and 1.1-1.6% decade<sup>-1</sup> in the tropics (WMO, 2022; Godin-Beekmann et al. 2022; SPARC/IO3C/GAW, 2019). These  
42 increases are consistent with model simulations showing that they arise from a combination of decreasing ozone-  
43 depleting substances concentrations and upper-stratospheric temperatures, driven by increasing CO<sub>2</sub> (WMO, 2022).  
44 Conversely, there has been an observed decrease in lower stratospheric ozone in the mid-latitudes since 1998 which  
45 is mainly driven by natural atmospheric variability and transport processes (Benito-Barca et al. 2025), this leads to  
46 insignificant trends in total column ozone in some regions such as the northern mid-latitudes. There is also evidence  
47 from both observations and models for a small decrease in tropical lower stratospheric ozone over the same period of

48 1-2% decade<sup>-1</sup>. This decrease has a large uncertainty of  $\pm 5\%$  decade<sup>-1</sup>, but is consistent with climate change-driven  
49 acceleration of the large-scale circulation and has a small impact on total column ozone (WMO, 2022).

50  
51 In order to detect such ozone changes, and to continue to monitor the health of the ozone layer, long term, vertically  
52 resolved, global observations of stratospheric ozone are needed. The NOAA/NASA Ozone Mapping and Profiler Suite  
53 (OMPS) sensors are a series of satellite instruments that are designed to meet this need by providing both total ozone  
54 and profile measurements (Flynn et al., 2006). The OMPS consists of three different sensors: a nadir mapper (OMPS  
55 NM), a nadir profiler (OMPS NP) and a limb profiler (OMPS LP). The first OMPS was launched onboard the Suomi  
56 National Polar-orbiting Partnership (SNPP) satellite in 2011 and consisted of all three OMPS sensors (Kramarova et  
57 al., 2014). The second was launched onboard NOAA-20 in 2017 with just the NM and NP on board, and the third,  
58 which again consisted of all three sensors, was launched onboard NOAA-21 in 2022. Two more OMPS containing all  
59 3 sensors will be launched in the next decade providing decades of continuous ozone observations.

60  
61 The validation of remotely sensed observations is crucial, not only to give confidence in scientific conclusions drawn  
62 from their use, but to also build community trust in the data and thus encourage their wider use. For this reason, we  
63 need to compare the retrieved data to as many different sources of correlative observations as are available to us. In  
64 this study we validate OMPS LP version 2.6 ozone retrievals against ozone profile data from two solar occultation  
65 satellite instruments (SAGE III/ISS and ACE-FTS), limb emission satellite Aura MLS, the nadir viewing satellite  
66 OMPS NP, a set of ground-based ozonesondes, and the lidar at Mauna-Loa.

## 68 2. The OMPS Limb Profiler and retrieval description

69 The Ozone Mapping and Profiler Suite Limb Profiler (OMPS LP) is a series of satellite sensors that perform limb  
70 measurements of scattered solar radiation in the ultraviolet, visible and near infrared wavelengths (290 to 1000 nm)  
71 (Kramarova et al. 2014) which allow for the retrieval of ozone profiles from the top of clouds up to 57 km. In order  
72 to increase the cross-track coverage, the OMPS LP instrument has three observation slits separated horizontally by  
73 4.25° (~250 km), but in this study, we only consider measurements from the center (nadir) slit, as this is the data that  
74 is currently released to the public (Kramarova 2023). The first OMPS LP was launched onboard the SNPP satellite in  
75 October 2011 and began operational observations in April 2012, it is this instrument that will be the focus of this  
76 paper.

77  
78 OMPS LP ozone profile retrievals are described in Rault and Loughman (2013) and Kramarova et al. (2018). Recently  
79 the retrieval algorithm was updated from version 2.5 to version 2.6. Several incremental improvements were made, as  
80 detailed in Kramarova et al. (2024), which include updated level 1 calibrations, an updated level 2 retrieval algorithm  
81 (including combining the UV and visible channels into a single retrieval) and improved data quality for OMPS LP  
82 version 2.6 ozone profile retrievals over version 2.5,. A filter was also introduced to remove profiles affected by the  
83 Hunga Tonga eruption in 2022-2023. This filter is based on retrieved aerosol extinction and results in gaps in OMPS  
84 LP ozone observations in the lower stratosphere (12.5-22.5 km) in the southern midlatitudes and tropics (45°S–20°N)  
85 that persist for several months after the eruption.

86 Validation of version 2.5 showed mean differences with correlative measurements of less than  $\pm 10\%$  between 18 and  
87 42 km, with a negative bias above 43 km and larger biases in the lower stratosphere and upper troposphere; there was  
88 also a positive drift of  $\sim 0.5\%/\text{yr}$  which was more pronounced above 35 km (Kramarova et al., 2018). Comparisons of  
89 version 2.6 retrievals with Aura MLS by Kramarova et al. (2024) found that the algorithm improvements have helped  
90 to reduce vertical oscillation seen in version 2.5 and negative biases above 45 km have been reduced. Mean biases  
91 compared to MLS are within  $\pm 10\%$  above 20 km and in many places less than  $\pm 5\%$ ; there has also been a reduction  
92 in the relative drifts between OMPS LP and MLS to less than  $0.2\%/\text{yr}$  in the upper stratosphere above 35 km  
93 (Kramarova et al., 2024).

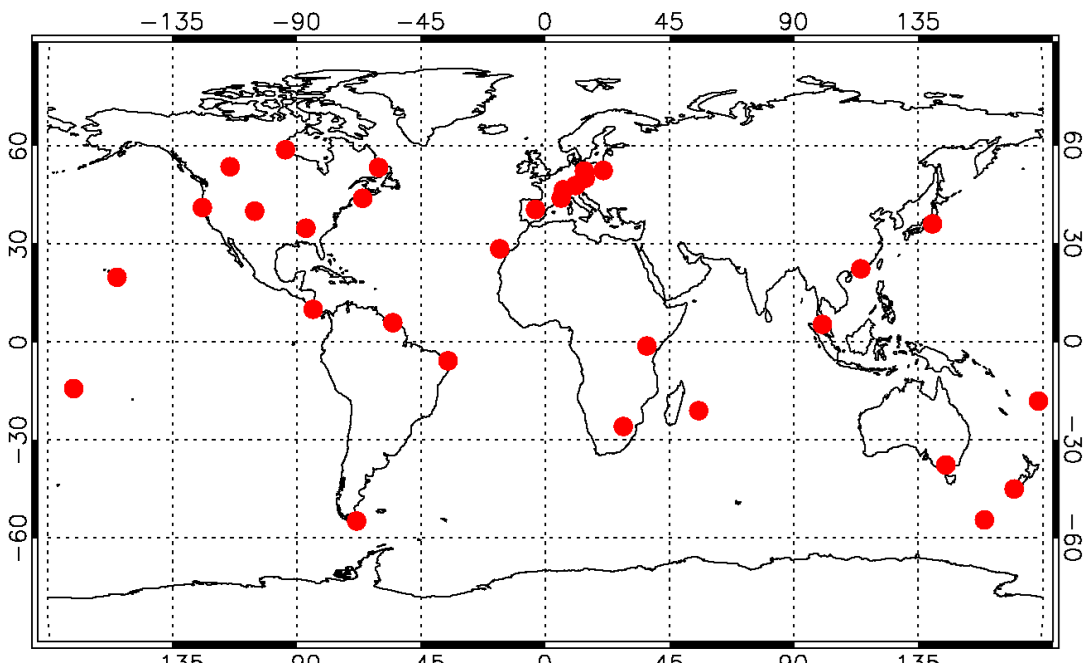
94  
95 This study focuses on the validation of OMPS LP version 2.6 ozone profile retrievals for the period April 2012 to  
96 April 2024. All OMPS LP data have been filtered using the suggested quality flags as described in the dataset readme  
97 document (Kramarova & DeLand, 2023).

100 **3. Correlative satellite and ground-based datasets**

101  
102 SNPP OMPS LP version 2.6 profiles have previously been compared to MLS (Kramarova et al., 2024). Since MLS  
103 will be decommissioned in the coming year we need to investigate alternative sources of correlative data with which  
104 to validate OMPS LP ozone profiles. This study builds on Kramarova et al. (2024) which compared OMPS LP version  
105 2.6 to MLS for the period 2012-2021 to include other sources of correlative data and extends the evaluation period to  
106 April 2024. Ozonesonde observations offer one such dataset, however the geographical, temporal and vertical (up to  
107 30 km) extent of the data is limited. Other satellite data are available, and although solar occultation instruments such  
108 as ACE-FTS and SAGE III/ISS may not provide such extensive spatial coverage as MLS, they are able to provide  
109 high vertical resolution ozone profiles at different latitude bands throughout the year, providing the opportunity for  
110 near global seasonal validation of OMPS LP ozone profiles.  
111

112 **3.1. Ozonesondes**

113 Ozonesondes provide high accuracy, in situ, ozone profile observations from the surface up to approximately 30 km  
114 altitude, however the data are spatiotemporally sparse. In this study we use data from 31 ozonesonde sites distributed  
115 throughout the globe; Figure 1 shows a map of sites used and table S1 lists the site names, data sources, principal  
116 investigator names and affiliations. Ozonesonde sites were selected for use based on continuity of data for the OMPS  
117 LP measurement evaluation period of April 2012 to April 2024. A recent study by Stauffer et al., (2022), which  
118 compared data from a network of 60 ozonesonde stations with satellite data, showed that when compared to Aura  
119 OMI, total column ozone was stable to within about  $\pm 2\%$  over an 18 year period, with similar results when compared  
120 to three other total column satellite instruments. When compared to MLS, stratospheric ozone from sondes agreed to  
121 within  $\pm 5\%$  from 50 to 10 hPa. The study concluded that overall, global ozonesondes network data are of high quality  
122 and stability.  
123

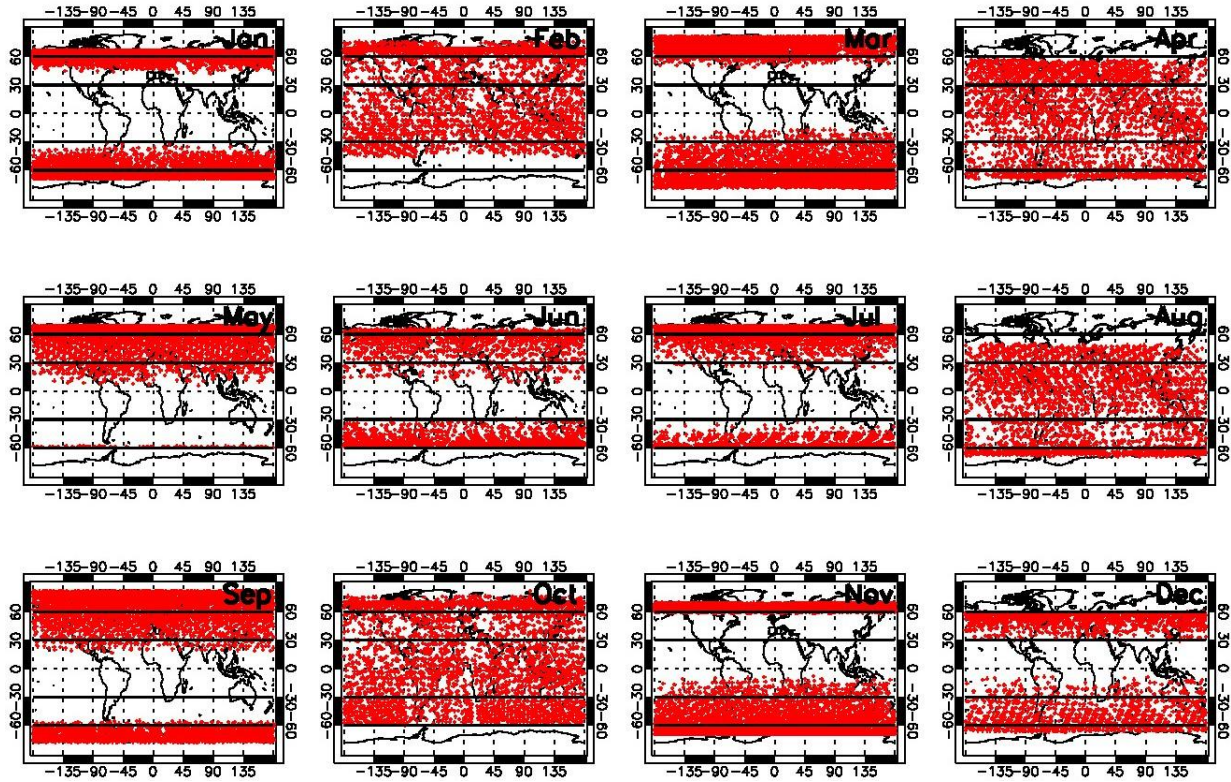


125  
126 **Figure 1: Location of ozonesonde sites used for validation of SNPP OMPS LP version 2.6 ozone retrievals.**  
127

128 **3.2. ACE-FTS**

129  
130 The Atmospheric Chemistry Experiment-Fourier Transform Spectrometer (ACE-FTS), is a solar occultation satellite  
131 instrument that makes measurements of ozone and other trace gases at sunrise and sunset (Bernath et al., 2005;

132 Bernath, 2017). ACE-FTS was launched onboard the Canadian Space Agency's SCISAT-1 satellite in 2003 and  
 133 therefore provides correlative data for the entire SNPP OMPS LP record. In this study we use ACE-FTS data version  
 134 5.2 (Bernath et al., 2025) and apply the quality flags of Sheese & Walker (2023). We only use observations co-located  
 135 with OMPS measurements (see Section 4), and since ACE-FTS only measures at sunset and sunrise, and its orbit is  
 136 optimized to provide coverage over polar mid and high latitudes, there are a limited number of co-located profiles to  
 137 use for the comparison with global OMPS LP observations, see Fig. 2. ACE-FTS version 5.2 ozone retrievals have  
 138 been validated against ozonesonde observations in a study by Zuo et al. (2024). These results show that ACE-FTS  
 139 ozone profiles have a general high bias in the stratosphere increasing with altitude up to ~10% at ~30 km, with  
 140 generally small insignificant drifts in the stratosphere (0-3%/decade). Comparisons with ozonesondes only extend up  
 141 to ~30 km, for higher altitudes, only previous versions have been validated against other satellite instruments.  
 142 Validation of ACE-FTS version 4.1 profiles shows that ACE-FTS ozone has a positive bias of 2-9% in the middle  
 143 stratosphere that is stable to  $\pm 0.5\%$ /decade, and a positive bias in the upper stratosphere that increases with altitude  
 144 up to ~15% and is stable to within  $\pm 1\%$ /decade (Sheese et al., 2022). The estimated precision for version 4.1 ozone  
 145 retrievals is on the order of ~5-10% (Sheese et al., 2022).  
 146

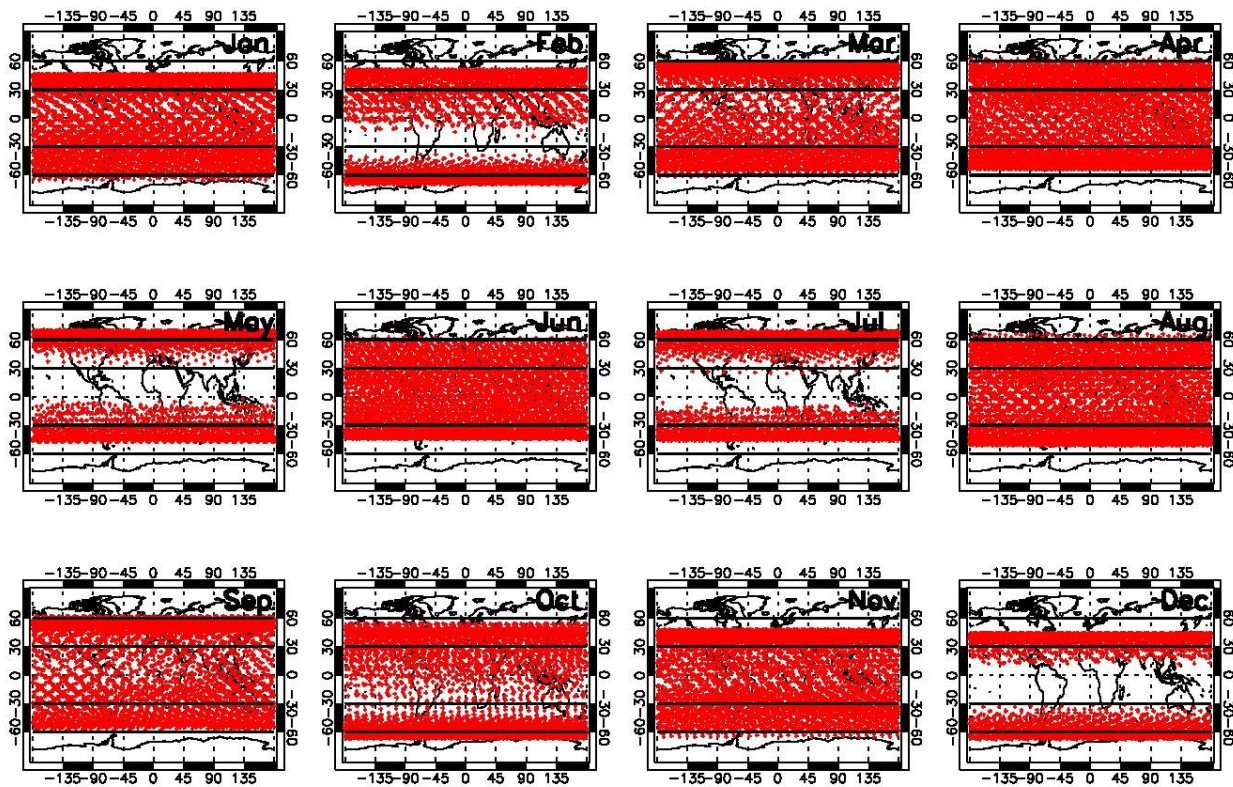


147  
 148 Figure 2: Co-located ACE-FTS observations by month for the period 2012-2024.  
 149

### 150 3.3. SAGE III/ISS

151 Like ACE-FTS, the Stratospheric Aerosol and Gas Experiment (SAGE) III, is a solar occultation instrument that  
 152 makes measurements of ozone profiles at sunrise and sunset (Cisewski et al., 2014). SAGE III/ISS was docked to the  
 153 International Space Station (ISS) in 2017 and began collecting data in June, thus providing nearly 8 years of correlative  
 154 data to compare with OMPS LP. In this study we use SAGE III/ISS ozone data version 6.0 (SAGE III/ISS data product  
 155 user's guide, 2025). Owing to the fact that SAGE III/ISS is a solar occultation instrument and is on board the ISS, it  
 156 provides limited global coverage which varies seasonally, doesn't extend north/south of approximately 70 degrees  
 157 latitude, and has more frequent sampling of the tropics. Again we only use observations co-located with OMPS  
 158 measurements (see Section 4), therefore, as with ACE-FTS there are a limited number of co-located global profiles  
 159 with which to compare with OMPS LP, see Fig. 3. The last version of SAGE III/ISS ozone to be validated was v5.1  
 160 (Wang et al., 2020). Those results showed that SAGE III/ISS ozone has a precision of ~3% in the 20-40 km altitude  
 161

162 range which degrades due to lower signal-to-noise ratios at higher and lower altitudes, reaching ~10-15% in the upper  
 163 stratosphere/lower mesosphere (~55 km) and ~20-30% near the tropopause. The mean biases when compared to  
 164 ozonesondes, lidars and other satellite correlative measurements are less than 5% for ~15-55 km in the mid-latitudes  
 165 and ~20-55 km in the tropics, increasing to 10% near the tropopause and to 15% at 60 km. Subsequent changes applied  
 166 in version 5.3 to the ozone retrievals have led to degraded precision (5% in the mid/lower stratosphere), but increased  
 167 vertical resolution, a reduction in low-altitude biases and a slight reduction in random noise. Changes made to version  
 168 6 have led to an increase in retrieved ozone of around 3% due to switching to the new ozone absorption coefficients  
 169 (SAGE III/ISS data product user's guide, 2025).  
 170



171  
 172 **Figure 3: Co-located SAGE III/ISS observations by month for the period 2017-2024.**  
 173

174 **3.4. MLS**

175  
 176 The Microwave Limb Sounder (MLS, Waters et al., 2006) provides global profile observations of ozone and other  
 177 trace species. MLS was launched on board the Aura satellite in 2004 and so provides correlative data for the entire  
 178 OMPS LP record to date. In this study we use version 5 of MLS data (Livesey et al., 2022). Since OMPS LP only  
 179 measures during the day, we only use MLS daytime observations, we also filter MLS data using criteria recommended  
 180 by the MLS Team. Both SNPP and Aura are in similar orbits with very similar equator crossing times and so MLS  
 181 provides excellent co-located profiles for global comparisons with OMPS LP. MLS ozone profiles have a precision  
 182 of 2-4% in the 18-43 km altitude range and this rapidly degrades outside of this altitude range (Livesey et al., 2022).  
 183 The accuracy of MLS ozone profiles ranges from 5 to 10% in the 12-57 km altitude range (Livesey et al., 2022), which  
 184 is the altitude range of interest in this study. MLS exhibits drifts with respect to ground-based networks of 1.5-  
 185 2%/decade but with zero drift encompassed by the error bars, at least in the middle stratosphere, and so is not  
 186 statistically significant (Livesey et al., 2022).

187 **4. Comparison Methodology**

188

189 In this study we apply common coincidence criteria to all correlative data to match OMPS LP profile sampling. Our  
190 spatial coincidence criteria require profiles to be within  $\pm 2^\circ$  latitude and less than 1000 km distance from the OMPS  
191 profile. In order to maximise the number of comparison profiles, the only time criterion is that the profiles be on the  
192 same day. If more than one profile matches these criteria then the spatially closest profile is used. We analyse all  
193 profiles on the native OMPS LP coordinate system (number density/altitude), and do not account for the small  
194 differences in the vertical resolution of the different measurement systems. Both MLS and ACE report ozone  
195 concentrations in volume mixing ratio, in order to convert this to number density for comparison to OMPS we need  
196 temperature and pressure information. For MLS, we use GEOS-FPIT temperature and pressure, and for ACE we use  
197 temperature and pressure retrieved by ACE itself. No transformation is needed for SAGE III/ISS or ozonesonde data  
198 as these data are provided as ozone number density profiles, however these data are provided on different altitude  
199 grids to OMPS LP. Ozonesonde data are converted, where necessary, from volume mixing ratio to number density,  
200 and from pressure grids to altitude grids, using the pressures and temperatures reported in the original data files, these  
201 are then transformed onto the OMPS LP vertical grid via log-linear interpolation. SAGE III/ISS data are provided on  
202 a 0.5 km vertical grid and so no interpolation is needed, we simply select matching altitudes for comparison profiles.  
203

204 Stratospheric ozone exhibits diurnal variability, particularly above 30 km, which is both seasonally and latitudinally  
205 dependent. The OMPS LP is a solar scattering instrument with a 1:30 pm equatorial crossing time that makes  
206 observations in the sunlit portion of the Earth, whereas both ACE-FTS and SAGE III/ISS are solar occultation  
207 instruments that measure ozone only at sunrise and sunset. We must therefore take into account the effects of any  
208 diurnal changes in ozone between the OMPS LP observations and those of ACE-FTS and SAGE III/ISS. This is  
209 achieved through the use of the Goddard Diurnal Ozone Climatology (GDOC) which is used to adjust both ACE-FTS  
210 and SAGE III/ISS observations to the measurement time of OMPS LP. Diurnal adjustment using this climatology has  
211 been shown to reduce biases above 30 km (Frith *et al.* 2020).

212 Initially matched profiles were averaged into 5 degree zonal means for comparison. In addition, owing to limited data  
213 coverage from correlative solar occultation satellite observations (see Figs. 2 & 3), the data were further averaged into  
214 3 wide latitude bands to increase the number of observations in each bin for comparison statistics. These bands are  
215 30°S-60°S, 30°S-30°N and 30°N-60°N and exclude the polar regions.

## 218 5. Results

### 219 5.1. Global profile comparisons

220 The mean biases for SNPP OMPS LP ozone retrievals compared to matched correlative measurements are shown in  
221 Fig. 4. The upper panels a-c of figure 4 show zonal mean biases ( $5^\circ$  latitude bins) between OMPS LP, ACE-FTS and  
222 MLS as a function of altitude for the period 2012-2024 (2017-2024 for SAGE III/ISS). Panels d-f of figure 4 show  
223 the mean biases for OMPS LP compared to all correlative measurement sources (ACE-FTS, SAGE III/ISS, MLS and  
224 ozonesondes) as a function of altitude for 3 wide latitude bands, averaged over the period 2012-2024 (except SAGE  
225 III/ISS, which is 2017-2024). The standard error of the mean for each comparison is also shown as horizontal bars,  
226 standard deviations for these comparisons are shown in Fig. S1 in the supplemental material. SNPP OMPS LP version  
227 2.6 ozone shows very good agreement with all correlative data sources between  $\sim 20$  and 50 km at all latitudes, with  
228 differences of less than  $\pm 10\%$ , and between 20 and 45 km the differences between OMPS and MLS, and OMPS and  
229 SAGE III/ISS are less than 5% in the tropics and southern mid-latitudes. Above 50 km, at all latitudes, the agreement  
230 is still on the order of 10% or better, but differences with SAGE III/ISS and ACE-FTS start to increase with increasing  
231 altitude above 55 km. This is consistent with the SAGE III/ISS and ACE-FTS validation results which show that both  
232 instruments have an increasing positive bias in the upper stratosphere (Wang *et al.*, 2020 and Sheese *et al.*, 2022). It  
233 is worth noting that without applying a diurnal correction to the ACE-FTS and SAGE III/ISS data the biases relative  
234 to these datasets are even larger by up to 10%.

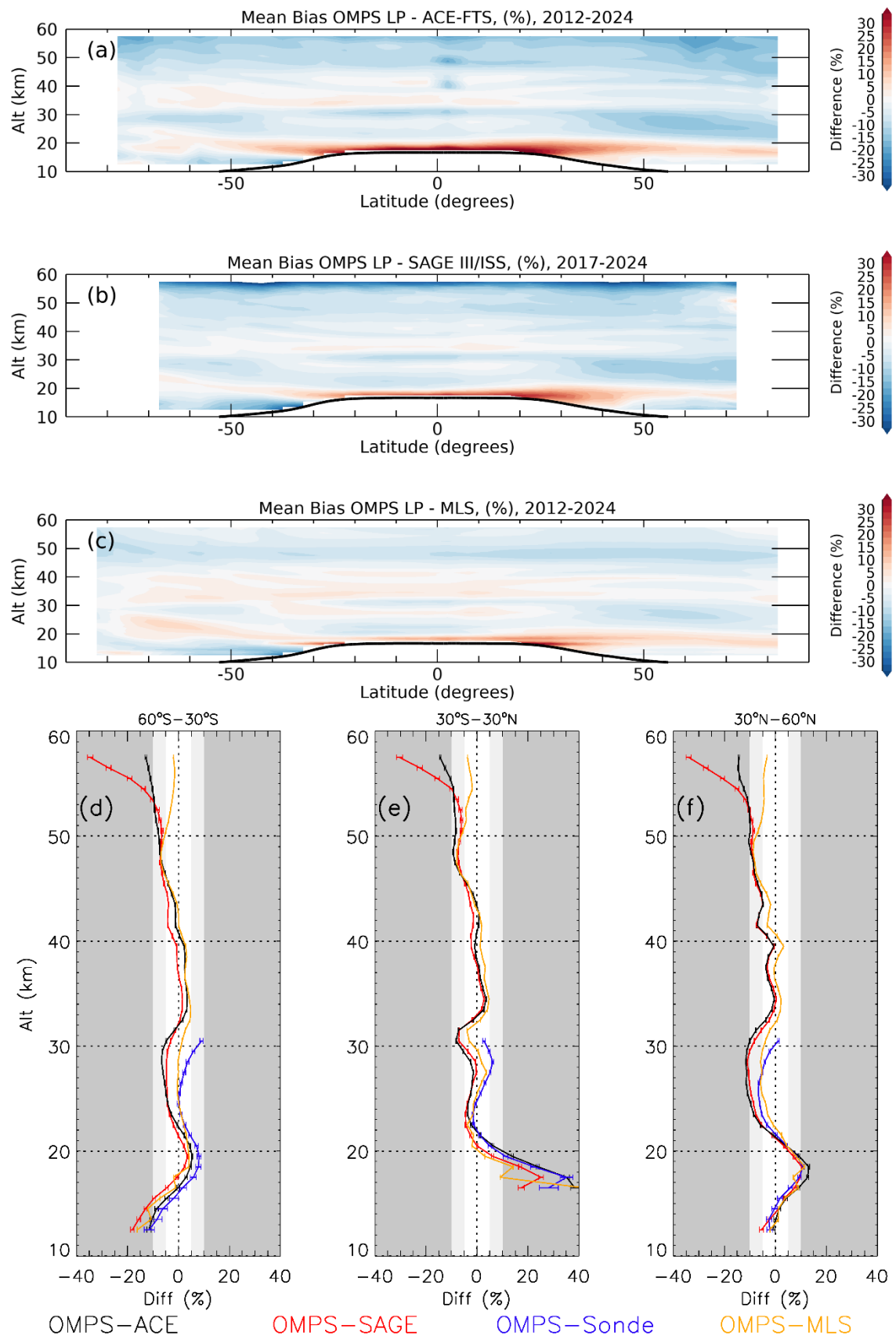
235 Below 20 km, the agreement between OMPS LP and correlative measurements varies by latitude, with larger positive  
236 biases in the Upper Troposphere Lower Stratosphere (UTLS) layer ( $\sim 15$  to 20 km) between approximately  $40^\circ$  South  
237 and  $40^\circ$  North. In the southern mid-latitudes OMPS LP agrees to within  $\sim 12\%$  between 12 and 20 km when compared  
238 to ACE-FTS, MLS and sondes, but shows slightly larger differences with SAGE III/ISS below 15 km. Below 20 km  
239

241 in the northern mid-latitudes, the biases between OMPS LP and all correlative measurements are comparable, and  
242 range from a positive bias of  $\sim 10\%$  at 18 km down to a small negative bias of  $< 5\%$  at 12 km.

243  
244 Overall, SNPP OMPS LP version 2.6 ozone profile biases do exhibit some vertical structure, with negative biases in  
245 the lowest part of the profile ( $< 15$  km), followed by a positive bias up to  $\sim 20$  km, then a negative bias again up to  $\sim 32$   
246 km, then a positive bias up to 40 km and then negative again above 40 km. This vertical pattern is somewhat latitude  
247 dependent, with the low altitude negative bias being stronger in the tropics and southern hemisphere, and the positive  
248 bias observed between  $\sim 32$  and 40 km not present at latitudes north of  $40^\circ\text{N}$ . However, almost all the biases when  
249 compared to correlative data from other satellite instruments (ACE-FTS, SAGE III/ISS and MLS) fall within the  
250 reported biases and precisions of those instruments. These biases represent an improvement over those observed  
251 between OMPS LP version 2.5 and MLS, with the largest reduction in biases seen below 31 km, where LP retrievals  
252 primarily rely on the visible triplet (Kramarova et al., 2024), there is also a reduction in vertical oscillations seen in  
253 version 2.6 compared to version 2.5, particularly where the retrieval switches between UV and visible wavelengths  
254 (approximately 28-32 km).

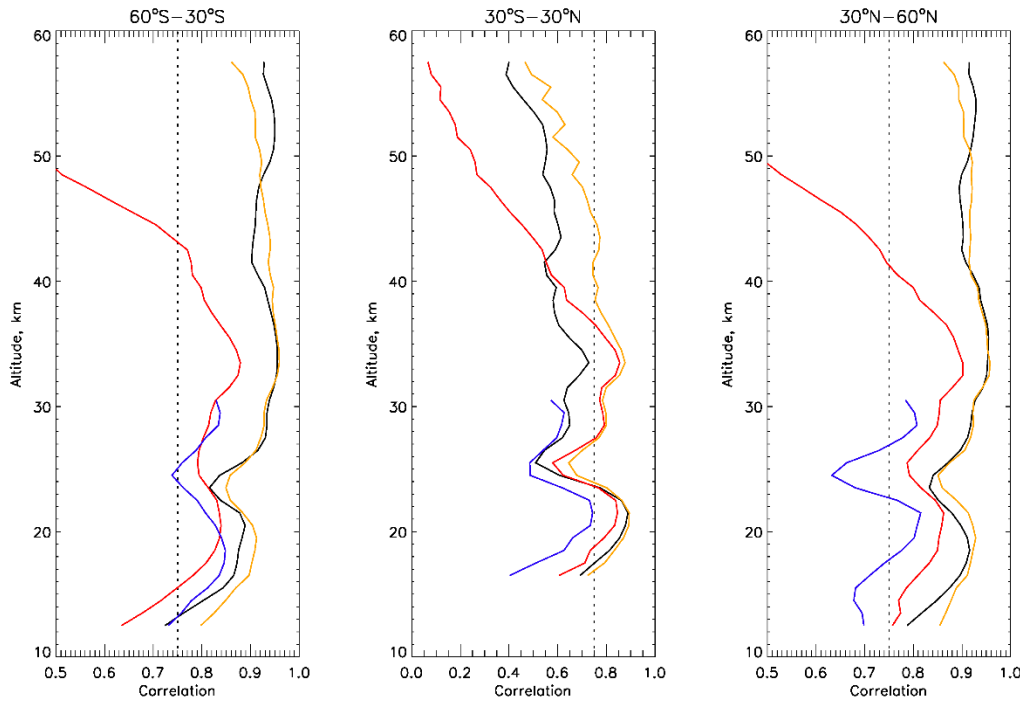
255  
256 Figure 5 shows vertical profiles of correlation coefficients between OMPS LP and matched correlative observations  
257 for 3 wide latitude bands. In the mid-latitudes correlations of approximately 0.9 are seen between OMPS LP and ACE-  
258 FTS and OMPS LP and MLS at most altitudes, and approximately 0.8 between OMPS LP and SAGE III/ISS between  
259 15 and 40 km. Above 40 km the correlation with SAGE III/ISS drops rapidly reaching less than 0.5 at around 50 km,  
260 indicating a spread in the biases at higher altitudes, this is also evident in the standard deviations of the profile  
261 comparisons shown in Fig. S1. This is consistent with degraded precision and increased noise for SAGE III/ISS  
262 measurements above 40 km as noted by Wang et al., (2020). It should be noted that, although we interpolate SAGE  
263 III/ISS observations from a 0.5 km to a 1 km vertical grid, we have not degraded the SAGE III/ISS profiles down to  
264 the resolution of OMPS LP, and this may also contribute to the lower correlations at higher altitudes.

265  
266 In the tropics, correlations between OMPS LP and MLS are around 0.8 up to 45 km dropping with increasing altitude  
267 to 0.5 at 57 km, correlations with SAGE III/ISS are approximately 0.8 up to 37 km and then drop with increasing  
268 altitude to 0.1 at 57 km. Correlations with ACE-FTS are between 0.4 and 0.8 throughout the entire vertical range with  
269 a stronger correlation below 25 km. The drop in correlations seen at around 25 km at all latitudes and against all  
270 correlative sources is likely because this is where ozone density peaks and it's variability is lower leading to weaker  
271 correlations. The correlations between OMPS LP and MLS and OMPS LP and ACE-FTS are improved at all altitudes  
272 and latitudes for version 2.6 over version 2.5, with the largest improvement seen in the tropical lower stratosphere  
273 where correlations between version 2.6 and MLS and ACE-FTS are greater than 0.8, whereas version 2.5 correlations  
274 were less than 0.7 compared to ACE-FTS and peaked at 0.8 compared to MLS (Kramarova et al., 2018).



278  
279  
280  
281  
282  
283  
284  
285

**Figure 4: Profile differences between OMPS LP and matched correlative satellite and ground-based observations.** Panels (a-c) show zonal mean differences between OMPS LP and ACE-FTS, OMPS LP and SAGE III/ISS and OMPS LP and MLS on a 5° latitude grid. Panels (d-f) show mean profile differences between OMPS LP and ACE-FTS (black), OMPS LP and SAGE III/ISS, OMPS LP and ozonesondes (blue) and OMPS LP and MLS (Orange) for 3 wide latitude bands, the horizontal bars show 2 times the standard error of the mean (SEM), the white area indicates differences less than 5%, the light grey area 5-10% and the dark grey area represents differences greater than 10%, only data above the tropopause are shown.



286  
287  
288  
289

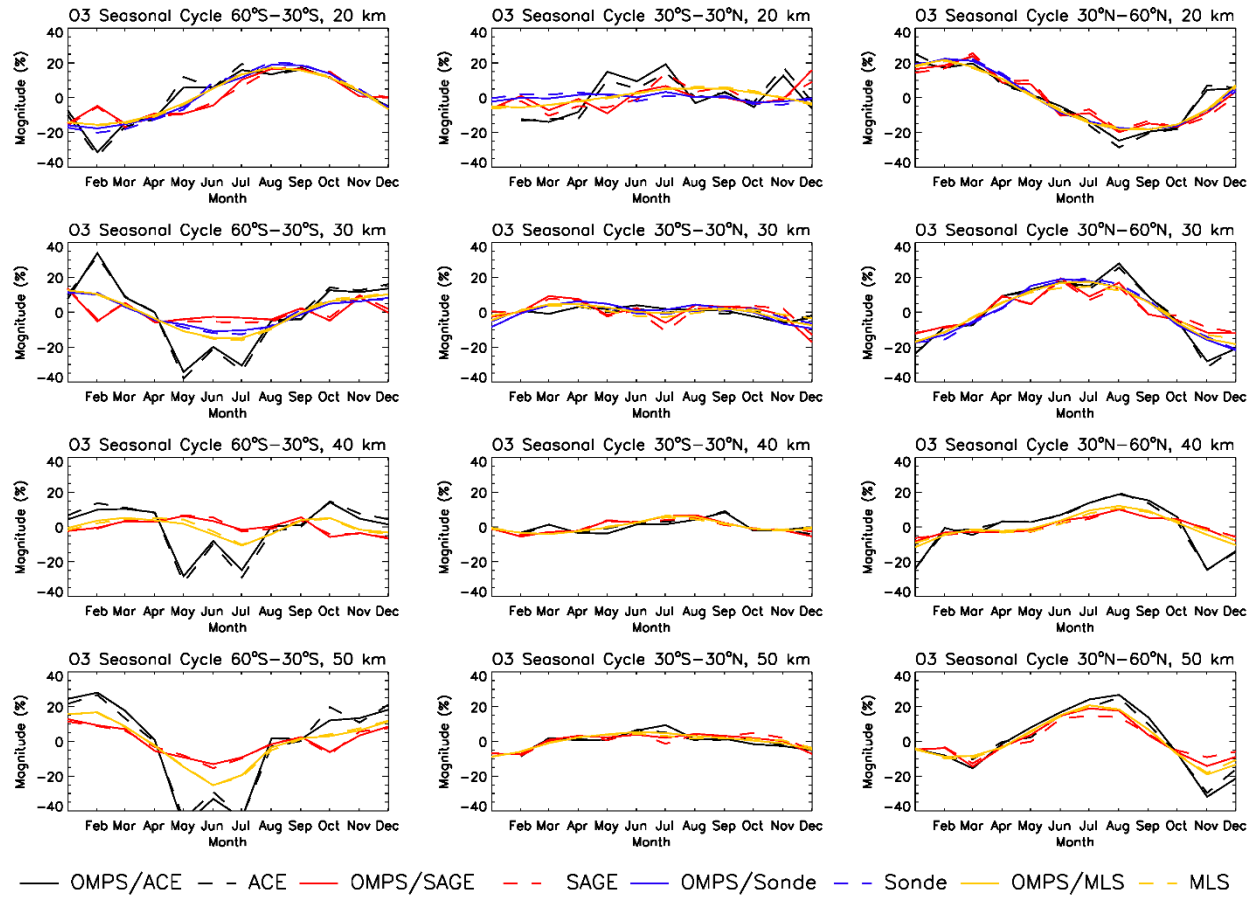
**Figure 5: Vertical profiles of correlation coefficients between OMPS LP and matched correlative observations for 3 wide latitude bands.**

## 290 5.2. Seasonal cycle

291  
292 To evaluate how well OMPS LP captures the seasonal cycle in ozone we compare the ozone seasonal cycle for each  
293 correlative dataset to co-located OMPS LP observations in 3 wide latitude bands as used previously. The seasonal  
294 cycle is calculated by taking each set of co-located OMPS LP and correlative data and subtracting the long-term mean  
295 from the monthly mean (for all years) for each latitude band. Figure 6 shows seasonal cycle comparisons between  
296 OMPS LP and all correlative measurements (ACE-FTS, SAGE III/ISS, MLS and sondes) at 4 altitudes (20,30,40 and  
297 50 km), the dashed lines represent the correlative observations seasonal cycles and the solid lines represent the co-  
298 located OMPS LP seasonal cycles. The shape of the seasonal cycle is generally consistent between OMPS LP and all  
299 3 correlative observation sources at all altitudes and latitudes. The seasonal cycle seen in ACE-FTS differs from the  
300 other instruments in the Southern Hemisphere at 30 km and above, this is likely due to the differences in sampling  
301 between ACE-FTS and the other instruments (see figures S2 and S3) as the OMPS LP co-located seasonal cycle has  
302 also changed from those for the dense coverage satellites (e.g., OMPS-MLS matches).

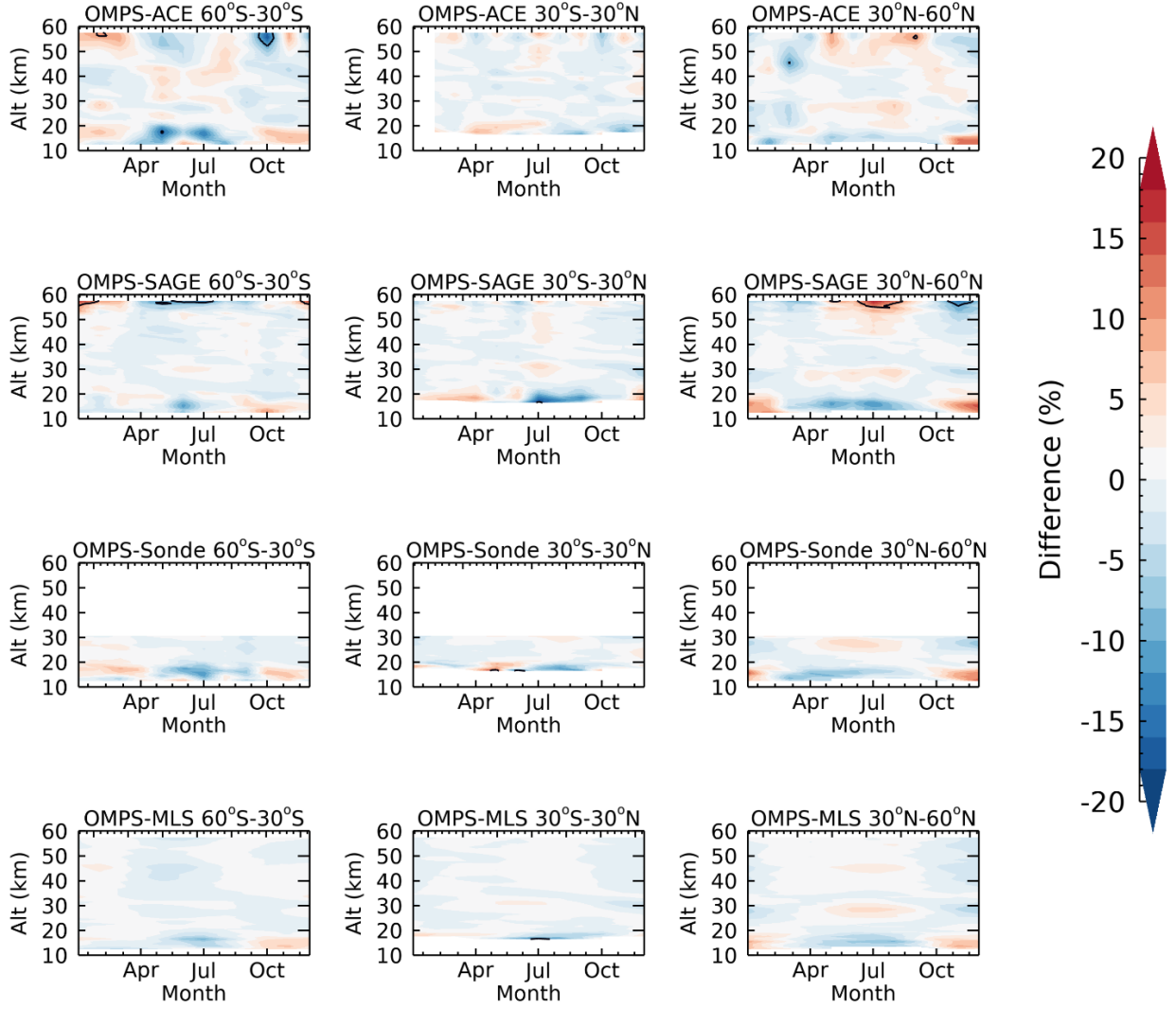
303  
304  
305 Figure 7 shows the seasonal cycle biases between OMPS LP and the correlative datasets (difference between solid  
306 and dashed lines in Fig. 6). There are small biases evident between the OMPS LP seasonal cycles and the seasonal  
307 cycles of correlate observations that vary by altitude and latitude, generally the biases are larger and noisier compared  
308 to ACE-FTS and SAGE III/ISS and are smaller and smoother compared to MLS, which may be a consequence of  
309 sampling differences. Below 20 km in the mid-latitudes there is a pattern to the seasonal biases that is consistent across

310 all correlative datasets, with a high bias seen in the early part of the year (January-March), followed by a negative bias  
 311 in the middle of the year (April-September) and then a positive bias towards the end of the year (October-December).  
 312 Despite the pattern, although not the magnitude, of these biases being consistent across all correlative sources they  
 313 are, however not statistically significant, as indicated by the absence of black contour lines in Fig. 7. At 30 km a  
 314 consistent small positive bias is seen between April and September in the northern mid-latitudes when compared to  
 315 all correlative sources that is not present at other latitudes, this bias is significantly smaller than a similar bias observed  
 316 in OMPS LP version 2.5 which was attributed to an unexpected thermal sensitivity issue with OMPS LP (Kramarova  
 317 et al., 2018; Jaross et al., 2014). However, in version 2.6 this bias is not statistically significant. Above 50 km larger  
 318 biases are seen relative to ACE-FTS and SAGE III/ISS in the mid-latitudes with negative biases observed in the  
 319 spring/summer months and positive biases in the fall/winter months, some of which are statistically significant as  
 320 indicated by the black contours in Fig. 7. However, these biases are not seen when compared to MLS. These results  
 321 show that there are no significant biases in the OMPS LP seasonal cycle.  
 322  
 323



324  
 325  
 326 **Figure 6: Seasonal cycle in co-located OMPS LP (solid lines) and correlative observations (dashed lines) calculated as**  
 327 **monthly mean deviations from the long-term annual mean in % calculated for each instrument independently. OMPS**  
 328 **seasonal cycles are calculated using a sub-set of matching profiles for each correlative instrument.**

329



330  
 331 **Figure 7: Seasonal cycle biases between OMPS LP and correlative observations, calculated as the differences between the**  
 332 **co-located OMPS LP seasonal cycle and the correlative observation seasonal cycle, black contours encompass biases that**  
 333 **are larger than 2 standard deviations.**

### 336 5.3. Long term stability of OMPS LP ozone

337  
 338 In order to assess the stability of OMPS LP version 2.6 ozone retrievals over time we calculate their drift with respect  
 339 to correlative measurements. Drifts are determined by calculating a linear fit for monthly mean deseasonalized co-  
 340 located differences between OMPS LP and each correlative dataset within each latitude band. Figure 8 shows the  
 341 calculated drifts in OMPS LP version 2.6 ozone relative to correlative measurements as a function of altitude above  
 342 the tropopause; the shaded areas represent 2 sigma for the linear fit.

343  
 344 Between 25 and 50 km OMPS LP exhibits a drift over the 2012-2024 period relative to MLS of less than 0.2 %/yr,  
 345 which is positive in the tropics and northern mid-latitudes (Fig. 8b-c), and negative in the southern mid-latitudes (Fig.  
 346 8a). The drifts relative to ACE-FTS and SAGE III/ISS at these altitudes remain predominantly negative at all latitude  
 347 bands and rise from less than -0.1 %/year at 25 km to -0.3 %/year at 50 km (Fig. 8a-c), except for the tropics where  
 348 SAGE III/ISS has a much larger drift at 50 km (-0.8 %/yr) than the other data sources (Fig. 8b), this is due to the  
 349 shorter time period where SAGE III/ISS and OMPS overlap (see discussion below). The drift relative to sondes  
 350 appears consistent with MLS and ACE-FTS in the mid-latitudes (Fig. 8a&c), but diverges in the tropics between 12

351 and 20 km (Fig. 8b), exhibiting a positive relative drift of up to +0.2 %/yr whereas the satellite observations show a  
352 small negative drift of up to -0.2 %/yr. The drifts of opposing signs observed between the different data sources  
353 indicate that OMPS LP exhibits no significant systematic drift between 25 and 50 km for the period 2012 to 2024.  
354

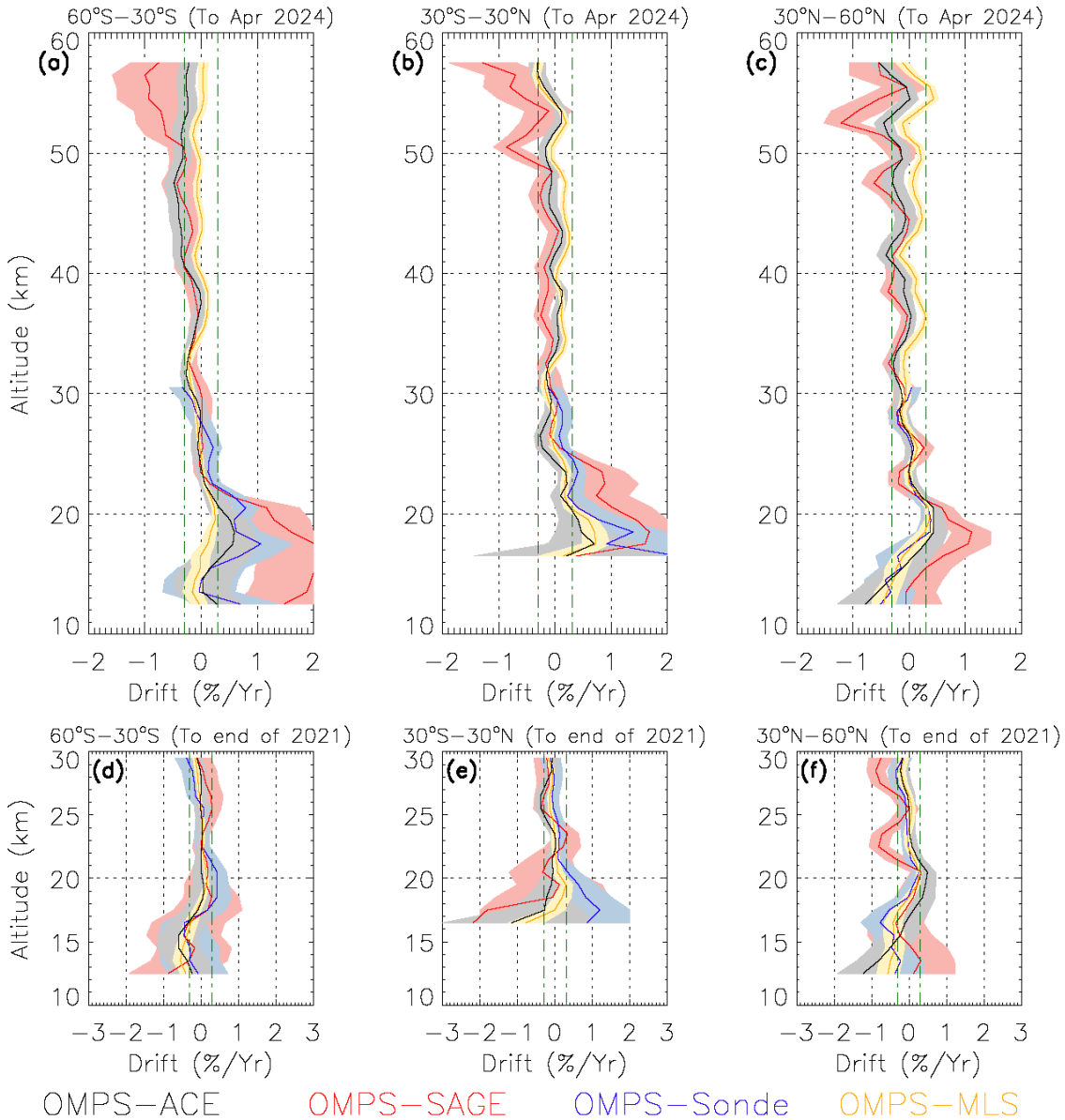
355 Above 50 km, in the tropics and southern mid-latitudes (Fig. 8a-b), drifts relative to MLS and ACE-FTS remain less  
356 than 0.2 %/year. In the northern mid-latitudes (Fig. 8c), the drift relative to MLS increases slightly and is positive (up  
357 to +0.4 %/yr) whereas the drift relative to ACE-FTS is negative (up to -0.4 %/yr). Again, the fact that the drifts relative  
358 to MLS and ACE-FTS are either close to or straddle the zero line, suggests that there is no significant systematic drift  
359 in OMPS LP at these altitudes over the 2012-2024 period.  
360

361 The eruption of the Hunga volcano in January 2022 caused problems for OMPS LP ozone retrievals because of high  
362 aerosol loading at 25 km and below, leading to anomalously high ozone being reported. A filter based on aerosol  
363 optical depth was implemented for OMPS LP ozone (Kramarova et al., 2024), this dramatically reduced the number  
364 of OMPS LP observations at altitudes below 25 km in the tropical and southern mid-latitude regions in the months  
365 following the eruption. However, even after this filter is applied, a higher than normal bias is still observed with  
366 respect to correlative observations in these regions that persists throughout 2022 and well into 2023. This positive  
367 anomaly is small when compared to MLS, but is larger when compared to ACE-FTS and is largest when compared to  
368 SAGE III/ISS as shown in Fig. S2 that demonstrates the time series of differences over the 2020-2025 period. Both  
369 SAGE III/ISS and ACE-FTS already had a limited number of observations in these latitude bands depending on the  
370 season, and with the reduction of OMPS LP observations the remaining number of matches in the low stratosphere  
371 for these two instruments is severely reduced from early 2022 to mid to late 2023 as shown in Fig. S3. The resulting  
372 drifts relative to ACE-FTS and particularly SAGE III/ISS below 25 km when calculated up to April 2024 appear to  
373 be erroneously large, especially in the tropics and southern mid-latitudes. For these reasons, for altitudes below 25  
374 km, we will focus on drifts calculated up to the end of 2021 only, which can be found in panels (d-f) in Fig. 8.  
375

376 Between 20 and 25 km OMPS LP exhibits a drift of less than  $\pm 0.3$  %/yr relative to ACE, MLS and sondes over the  
377 period 2012-2021 (Fig. 8d-f), with the largest drifts seen at 25 km in the tropics relative to ACE (Fig. 8e) and at 20  
378 km in the southern mid-latitudes relative to sondes (Fig. 8d). In the tropics and southern mid-latitudes (Fig. 8d-e) the  
379 drifts relative to different data sources straddle the zero line indicating no systematic drift for the time period 2012-  
380 2021, in the northern mid-latitudes the drifts are generally all less than 0.3%/yr and positive. Below 20 km, for the  
381 period 2012-2021, in the mid-latitudes (Fig. 8d&f) the drifts relative to all data sources shows the same structure and  
382 start out positive ( $\sim +0.2\%$ /yr), but then show an increasing negative trend with decreasing altitude which peaks at  $\sim$   
383 0.6%/yr at around 15 km before improving at the bottom of the profile (except for ACE-FTS in the northern  
384 hemisphere), with larger drifts seen at lower altitudes in the northern hemisphere. In the tropics there is a large spread  
385 in the drifts relative to the four different data sources. The drifts relative to ACE-FTS and MLS are similar and those  
386 relative to SAGE III/ISS and sondes have larger errors at these altitudes. ACE-FTS, SAGE III/ISS and MLS all show  
387 a negative drift whereas the drift relative to sondes is positive.  
388

389 These results represent an improvement in the long-term stability of OMPS LP ozone retrievals for version 2.6 over  
390 version 2.5, with a reduction in drifts at all altitudes, particularly in the upper stratosphere where version 2.5 exhibited  
391 drifts of 0.5-1%/yr (Kramarova et al., 2018). The observed drifts and the spread in drifts relative to different correlative  
392 data sources indicates that there is no significant systematic drift in OMPS LP version 2.6 above 20 km.  
393

394 The drifts relative to SAGE III/ISS have larger magnitudes, sigmas, and different vertical structures to those of other  
395 correlative measurements, particularly above 50 km and below 25 km. This is due to the shorter time period available  
396 for OMPS LP-SAGE III/ISS comparisons. Once recalculated, the drifts relative to ACE-FTS and MLS above 50 km  
397 and below 25 km exhibit similar magnitudes and vertical structures to that of SAGE III/ISS (Fig. S5). Analysis of the  
398 time series of differences between OMPS LP and MLS in the 30°N-60°N latitude band for several altitudes over the  
399 time period 2012 to 2024 (Fig. S6) show low frequency changes in ozone differences. Because of this the drifts for  
400 the periods 2012-2024 and 2017-2024 are quite different with mostly negative drifts for the period 2017-2024,  
401 however when we estimate the drift for the whole time period of 2012-2024 the drifts are much smaller. These time-  
402 dependent changes in LP ozone are being investigated by the OMPS LP team, who also see time dependent changes  
403 in radiance residuals (differences between calculated and measured radiances) at wavelengths that are not used in the  
404 ozone retrieval that coincide with observed changes in ozone. Investigation of this behavior in other LP slits (not  
405 shown here) suggest that this is not related to a drift in altitude registration. One possible explanation under  
406 investigation is a potential shift in wavelength registration.



407  
 408 **Figure 8: Relative drifts for OMPS LP version 2.6 ozone in % per year relative to correlative observations, calculated using**  
 409 **deseasonalized data from April 2012 to April 2024 for panels (a-c) and April 2012 to December 2021 for panels (d-f), except**  
 410 **for SAGE III/ISS for which data starts in June 2017. Shaded areas show 2 sigma for the linear fit, only data above the**  
 411 **tropopause is shown. The vertical dashed-dotted lines indicate a drifts of 0.3%/year, the WMO stability threshold for**  
 412 **stratospheric ozone trend studies (WMO 2022).**

413  
 414  
 415  
 416  
 417  
 418  
 419  
 420

## 6. Comparisons With Other Data Sources

415 In the future we won't be able to rely on having correlative satellite data with either both high vertical resolution and  
 416 dense global sampling such as MLS, or high vertical resolution and limited global sampling such as SAGE III/ISS or  
 417 ACE-FTS, as both MLS and SAGE III/ISS are scheduled to end operations in the near future and ACE-FTS is already  
 418 long past its original planned mission lifetime. With no replacement missions for these instruments likely in the near  
 419 future we will need to use other sources of correlative data with which to validate OMPS LP ozone retrievals in  
 420 addition to ozonesondes. Here we investigate the use of lidar data and lower vertical resolution nadir satellite data.

421

422 **6.1. Mauna Loa Lidar**

423

424 One other source of high vertical resolution ozone profile measurements is ground-based lidar observations, of which  
425 there are a limited number of stations located around the globe. Although the global coverage gained from lidar  
426 observations is significantly lower than that of ozonesondes, lidars are able to observe ozone up to higher altitudes  
427 than sondes (up to 50 km), therefore a combination of lidars and ozonesondes may provide a useful dataset for  
428 validation of OMPS LP high vertical resolution ozone profile retrievals, albeit with limited global coverage. Here we  
429 will compare to the Mauna Loa lidar station (MLO). The MLO lidar measures vertical ozone profiles from 15-50 km  
430 at night, several times a week, with a vertical resolution of ~1 km near the ozone peak (~25 km) which decreases to  
431 ~3 km at the bottom of the profiles and to 8-10 km at the top of the profiles (Leblanc and McDermid, 2000). The  
432 typical instrumental error is a few percent at the ozone peak and increases to 10-15% at ~15 km and to more than 40%  
433 above 45 km (Leblanc and McDermid, 2000).

434

435 In this study we utilize MLO lidar ozone data for the period April 2012 to December 2022 to evaluate OMPS LP  
436 version 2.6 ozone retrievals and compare these results to those of coincident MLS and ozonesonde comparisons to  
437 OMPS LP at this location. Figure 9 shows mean profile differences between OMPS LP and MLO lidar data together  
438 with collocated differences between OMPS LP and MLS and between OMPS LP and ozonesondes launches from the  
439 Hilo station. Between 20 and 45 km OMPS LP exhibits the same vertical structure in biases compared to both the  
440 MLO lidar and MLS, with biases near zero between 20 and 25 km and between 40 and 45 km for both data sources.  
441 Between 25 and 40 km the bias compared to the MLO lidar (~5-10%) is larger than that with MLS (<5%), however  
442 between 23 and 30 km the biases with MLO and ozonesondes agree almost perfectly. Below 20 km the bias compared  
443 to the MLO lidar is less than 10%, which is much smaller than the bias compared to both MLS and ozonesondes,  
444 however the standard deviation of the MLO biases increases dramatically at these altitudes (see Fig. S4), likely as a  
445 result of increased measurement error, and encompass the observed MLS and ozonesondes biases. Above 45 km,  
446 again the MLO lidar and MLS biases differ, with the MLO biases being much smaller than MLS. This is also a region  
447 where the MLO lidar measurement error increases dramatically and so does the standard deviation of the mean  
448 differences, which again encompass the MLS biases.

449

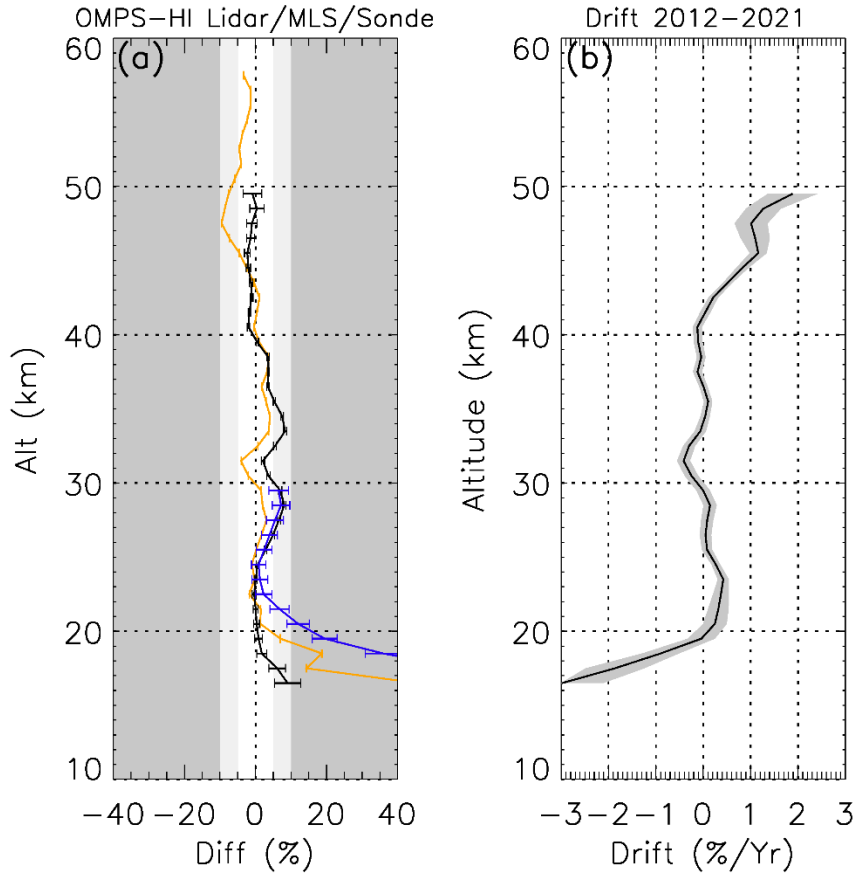
450 Panel (b) of Fig. 9 shows a profile of the relative drift of OMPS LP compared to the MLO lidar. This is determined  
451 by calculating a linear fit for monthly mean deseasonalized co-located differences for the time period of April 2012  
452 up to the end of 2021. Between 20 and 40 km the drift in OMPS LP relative to the MLO lidar is very close to zero  
453 (<±0.1%/yr), with the exception of a positive drift of less than 0.4%/yr between 20 and 24 km and a negative drift of  
454 less than -0.3%/yr at 32 km. Above 40 km the drift steadily increases with altitude reaching +1.2%/yr at 45 km and  
455 +1.8%/yr at 50 km, however as previously noted the lidar measurement error increases dramatically above 40 km as  
456 does the standard deviation of the differences, the vertical resolution of the lidar observations is also degraded to ~8-  
457 10 km at these altitudes and so any observed trends in OMPS LP with fine vertical structure, natural or otherwise,  
458 would likely lead to large drifts in the differences. Below 20 km drifts become increasingly negative increasing from  
459 ~0%/yr at 20 km to ~3%/yr at 16 km, again this is an altitude range with increased variability in the differences  
460 between the two datasets and increased lidar measurement error.

461

462 The results are broadly consistent with MLS and sonde comparisons in the same location, although the existence of  
463 some differences at higher and lower altitudes together with lidar observation error estimates, variability of differences  
464 and changes in vertical resolution lead us to conclude that such data is most useful for evaluation of OMPS LP ozone  
465 between 20 and 40 km. These results show that lidars can provide a useful dataset with which to evaluate OMPS LP  
466 high vertical resolution ozone profile retrievals once MLS data is no longer available.

467

468



469  
470 **OMPS–Lidar**    **OMPS–Sonde**    **OMPS–MLS**  
471 Figure 9: Mean profile differences and drifts between OMPS LP and Mauna Loa lidar observations. Panel (a) shows the  
472 mean profile differences between OMPS LP and lidar (black line), OMPS LP and MLS (yellow line), and OMPS LP and  
473 ozone sonde launches from Hilo (blue line), the horizontal bars show 2 times the standard error of the mean (SEM), the  
474 white area indicates differences less than 5%, the light grey area 5-10% and the dark grey area represents differences  
475 greater than 10%. Panel (b) shows the relative drift in % per year relative to lidar observations, calculated using  
476 deseasonalized data from 2012 to 2021. Shaded area shows 1 sigma for the linear fit, only data above the tropopause is  
477 shown.  
478  
479  
480  
481

482 **6.2. OMPS Nadir Profiler (NP)**  
483

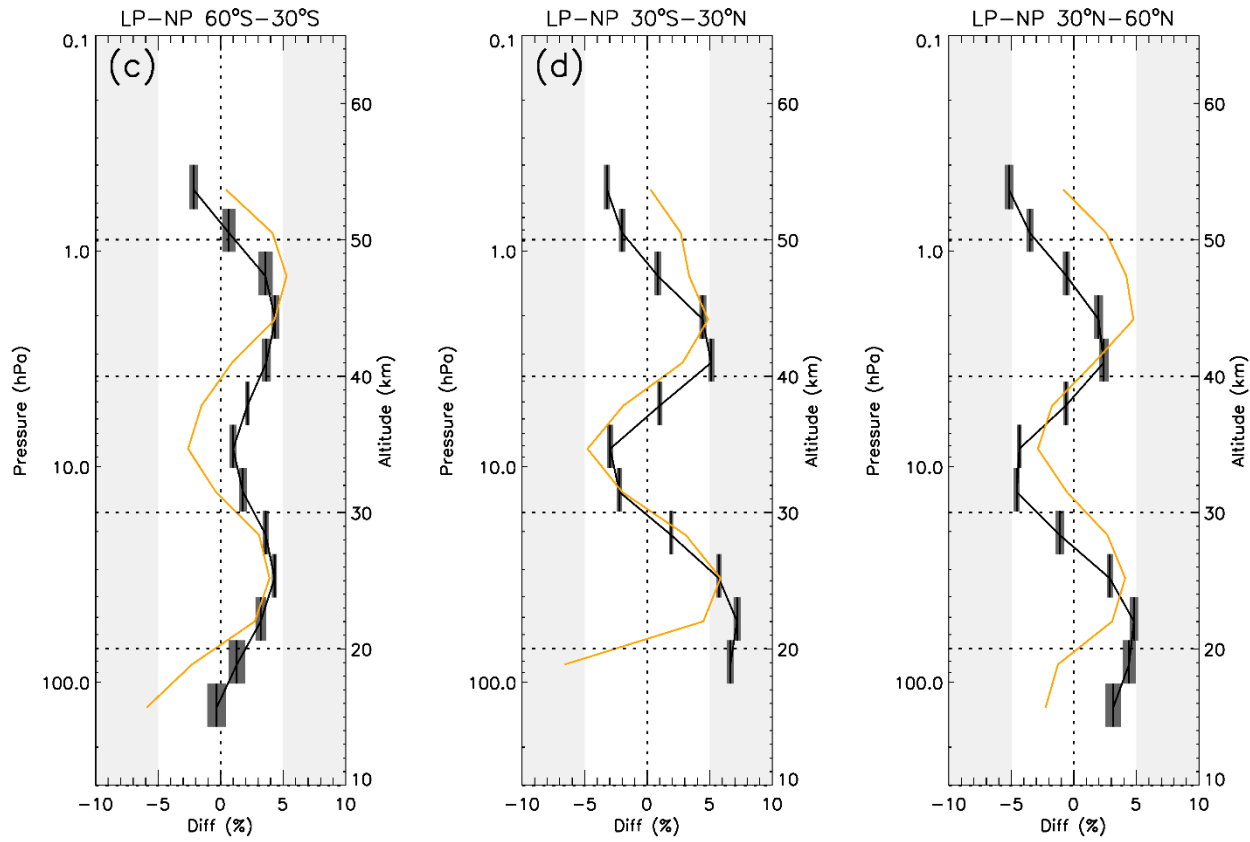
484 The OMPS nadir profiler (OMPS NP) is a nadir viewing instrument that is part of the OMPS suite of instruments and  
485 measures vertical profiles of ozone (McPeters et al., 2019) with limited vertical resolution (6-8 km). Despite the  
486 limited vertical resolution, it has a number of advantages as a correlative data source for the evaluation of OMPS LP  
487 ozone profiles. It is on board the same spacecraft as OMPS LP, and so its observations are near coincident with LP  
488 observations in both space and time, it is able to provide the same global coverage as OMPS LP (every 3-4 days),  
489 although its profiles are of low vertical resolution they do cover the full vertical range of OMPS LP ozone retrievals,  
490 and there will always be an NP instrument as part of the OMPS to provide data with which to compare. Ozone profile  
491 retrievals from SNPP OMPS NP have been demonstrated to agree with observations from NOAA-19 SBUV-2 to  
492 within  $\pm 3\%$  with an average bias of -1.1 % in the upper stratosphere and +1.1 % in the lower stratosphere (McPeters  
493 et al., 2019).  
494

495 In this study we utilize SNPP OMPS NP ozone profile for the period April 2012 to December 2024 to evaluate OMPS  
496 LP version 2.6 ozone retrievals. In order to compare OMPS LP and OMPS NP, OMPS LP profiles were first converted  
497 into partial ozone columns according to the OMPS NP pressure grid, the OMPS NP averaging kernels were then  
498 applied to the OMPS LP profiles to degrade them to the OMPS NP vertical resolution. Figure 10 shows mean profile  
499 differences between OMPS LP and OMPS NP averaged over the whole measurement time period for 3 wide latitude  
500 bands. In general, the biases relative to OMPS NP are less than 5% at all altitudes and all locations, with the exception  
501 of the tropical lower stratosphere (below 25 km). The biases for all locations show the same vertical oscillatory  
502 structure which is stronger in the tropics and northern mid-latitudes. This manifests as positive biases below ~28 km,  
503 negative biases between ~28 and ~36 km, positive biases between ~36 and ~46 km and negative biases above ~46 km  
504 for these two regions. Also shown in Fig. 10 are the mean profile differences between MLS and OMPS NP for the  
505 same latitude bands (yellow lines). Since the differences between MLS and OMPS NP exhibit the same oscillatory  
506 vertical structure as the differences between OMPS LP and OMPS NP, we can conclude that this vertical structure is  
507 an artifact of the OMPS NP measurements and not OMPS LP. With this in mind, the biases observed between OMPS  
508 LP and OMPS NP are consistent with those seen between OMPS LP and other correlative observations.  
509

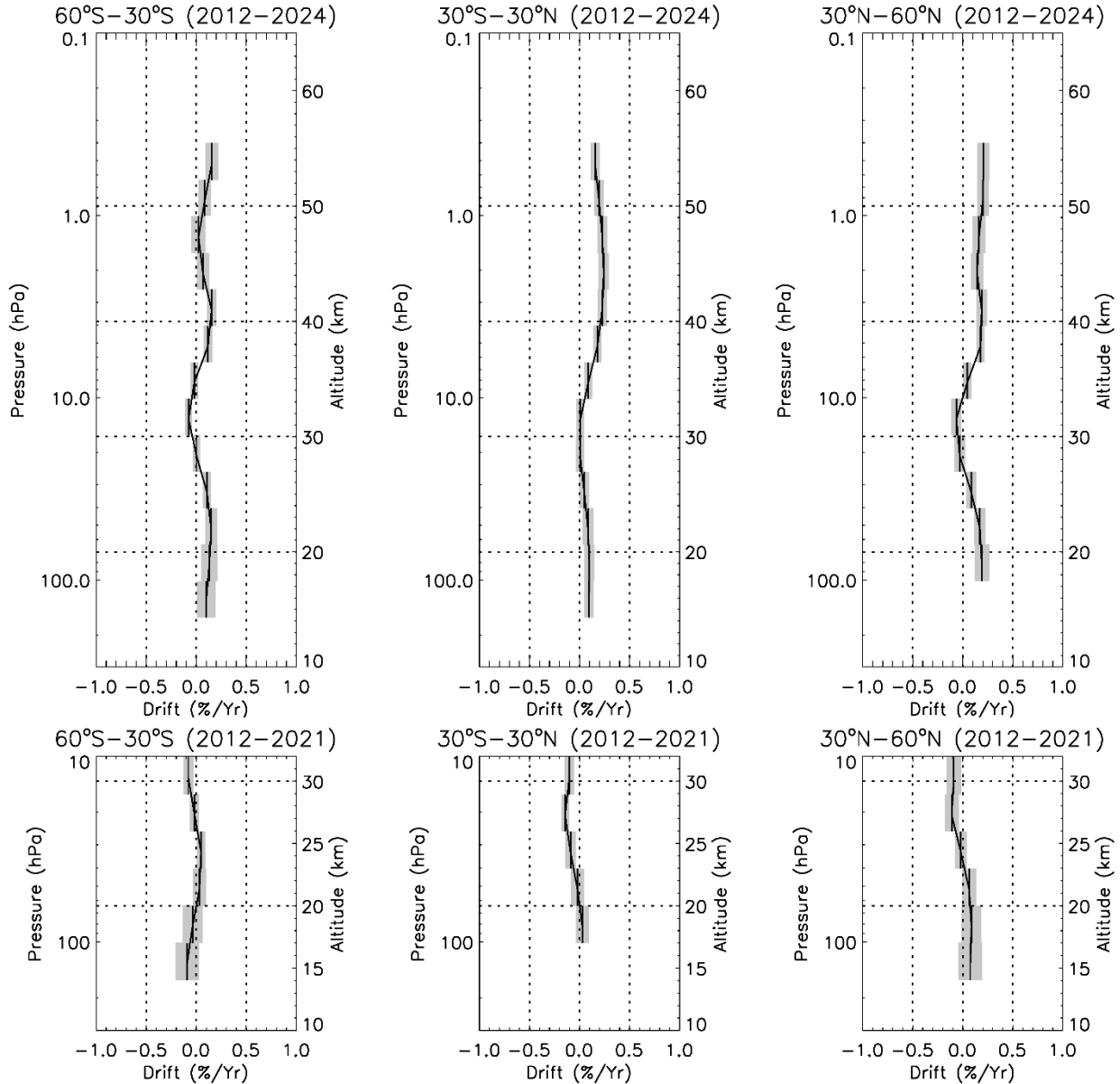
510 Figure 11 shows the drift of OMPS LP relative to OMPS NP. This is determined by calculating a linear fit for monthly  
511 mean deseasonalized differences for the time period of April 2012 up to the end of 2024 for altitudes above 25 km  
512 and up to the end of 2021 for altitudes below 25 km. Between ~13 and ~35 km the drift relative to OMPS NP is  
513  $<\pm 0.1\%/\text{year}$  in the mid-latitudes, and  $<\pm 0.2\%/\text{yr}$  in the tropics. Above 35 km the drift becomes positive in all latitude  
514 bands and increases up to  $0.3\%/\text{yr}$ . These drifts fall within the range of drifts seen when comparing OMPS LP with  
515 other correlative measurements.

516 These results suggest that OMPS NP is able to provide a useful dataset with which to globally evaluate OMPS LP  
517 ozone profiles, albeit with limited vertical fidelity. Bias calculations with OMPS NP introduce some oscillatory  
518 vertical structures which are a characteristic of the OMPS NP measurements and not OMPS LP. This should be taken  
519 into consideration when using OMPS NP to evaluate OMPS LP vertical profiles.  
520

521



522  
 523 **Figure 10: Mean profile differences between OMPS LP and OMPS NP (black) for 3 wide latitude bands, the horizontal**  
 524 **shading show 2 times the standard error of the mean (SEM), the white area indicates differences less than 5%, the light**  
 525 **grey area 5-10%. Also shown in yellow are mean profile differences between MLS and OMPS-NP. Only data above the**  
 526 **tropopause are shown.**



528  
 529 **Figure 11:** Relative drifts for OMPS LP version 2.6 ozone in % per year relative to OMPS NP, calculated using  
 530 deseasonalized data from April 2012 to December 2021. Shaded areas show 2 sigma for the linear fit, only data above the  
 531 tropopause is shown.  
 532  
 533

534 **7. Comparisons in Polar Regions**

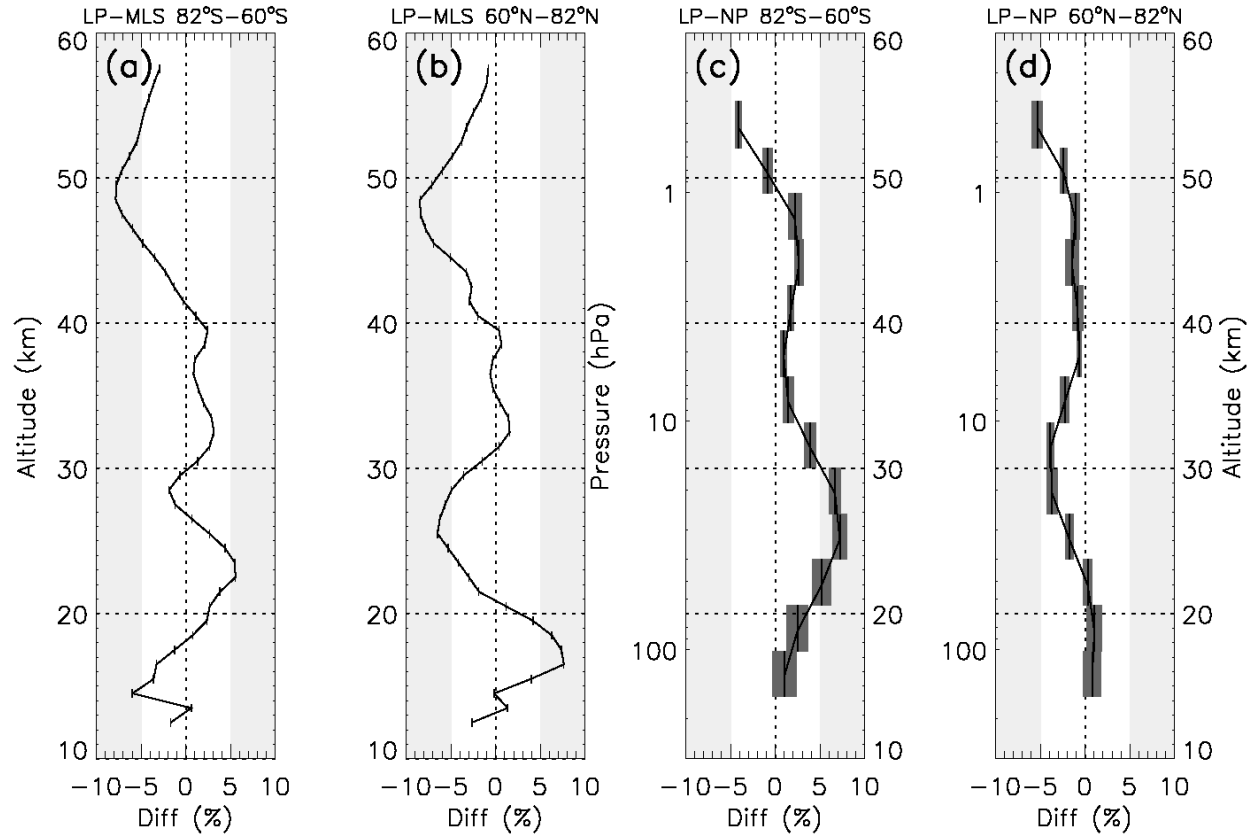
535 Previously, we limited our comparisons geographically to exclude polar regions (latitudes greater than 60°) owing to  
 536 sparse data in this region from all correlative data sources. However, MLS and OMPS NP have sufficient data  
 537 coverage that extends to latitudes greater than 60 degrees to evaluate OMPS LP ozone retrievals in these important  
 538 regions.  
 539

540 Figure 12 shows mean profile differences between OMPS LP and correlative observations in two wide polar latitude  
 541 bands, 82S–60S and 60N–82N. The biases relative to MLS are generally less than  $\pm 5\%$  except between 45 and 55 km  
 542 in the southern hemisphere where biases peak at  $-8\%$  at 48 km, in the northern hemisphere there are 3 altitude regions

543 where the bias relative to MLS exceeds  $\pm 5\%$ , 15-20 km, 23-30 km and 45-50 km, but those biases are still less than  
 544  $\pm 10\%$ . Compared to OMPS NP, LP biases are generally less than  $\pm 5\%$  except for approximately 25 to 30 km in the  
 545 southern hemisphere, and above  $\sim 52$  km in the northern hemisphere.

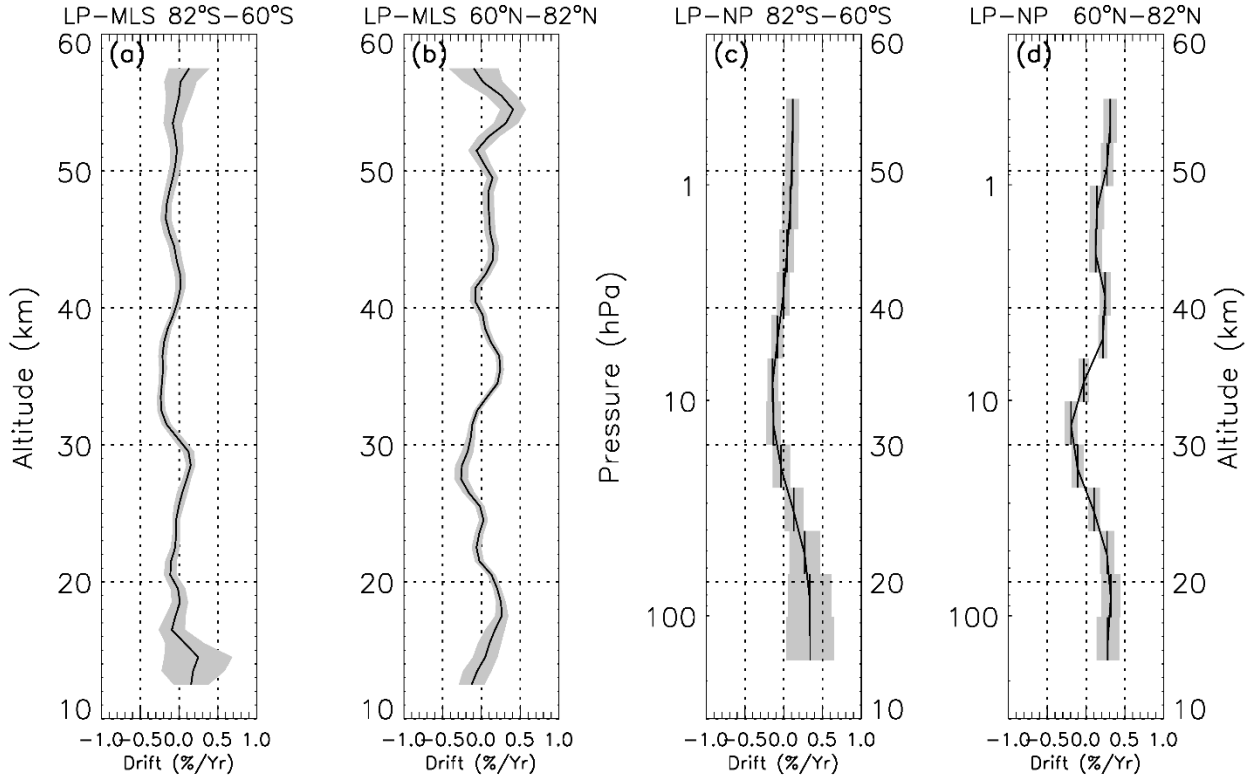
546  
 547 Figure 13 shows relative drift profiles between OMPS LP and correlative observations for the two polar regions. The  
 548 drift relative to MLS is less than  $\pm 0.2\%/\text{yr}$  at all altitudes in the polar regions except in the northern hemisphere at 18  
 549 km and between  $\sim 53$  and 55 km. Drifts of less than  $\pm 0.3\%/\text{yr}$  are seen relative to OMPS NP at all altitudes in both  
 550 polar regions, with drifts less than  $\pm 0.1\%/\text{yr}$  above 25 km in the southern hemisphere, and less than  $\pm 0.2\%/\text{yr}$  between  
 551 25 and 45 km in the northern hemisphere.

552  
 553  
 554



555  
 556 Figure 12: Mean profile differences between OMPS LP and correlative datasets in two polar latitude bands, 60S-90S and  
 557 60N-90N. Panels (a) and (b) show the mean profile differences between OMPS LP and MLS, the horizontal bars show 2  
 558 times the standard error of the mean (SEM). Panels (c) and (d) show the mean profile differences between OMPS LP and  
 559 OMPS NP, the horizontal shading show 2 times the standard error of the mean (SEM). The white area indicates differences  
 560 less than 5%, the light grey area 5-10% and the dark grey area represents differences greater than 10%, only data above  
 561 the tropopause are shown.

562  
 563



564  
565 **Figure 13: Relative drifts for OMPS LP version 2.6 ozone in % per year, calculated using deseasonalized data from April**  
566 **2012 to December 2024 for two polar latitude bands, 60S-90S and 60N-90N. Panels (a) and (b) show drifts relative to MLS.**  
567 **Panels (c) and (d) show drifts relative to OMPS NP. Shaded areas show 2 sigma for the linear fit, only data above the**  
568 **tropopause is shown.**

569

## 570 8. Conclusions

571  
572 In mid-2023 a new version of OMPS LP ozone profile retrievals, version 2.6, was released. Version 2.6 includes a  
573 number of incremental improvements in calibration, the retrieval algorithm and data quality. In order to evaluate this  
574 latest version of OMPS LP ozone profile data, we compared OMPS LP version 2.6 ozone retrievals against correlative  
575 data from other satellite instruments (MLS, ACE-FTS and SAGE III/ISS) and ozonesondes for the time period 2012-  
576 2024 in three wide latitude bands from 60°S to 60°N. Table 1 summarizes our results showing mean biases and drifts  
577 for 3 wide latitude bands (30°S-60°S, 30°S-30°N and 30°N-60°N) at 5 km altitude intervals.

578  
579 Our results show very good agreement between OMPS LP and all correlative data sources between 15 and 50 km at  
580 all latitudes with differences of less than 10%, with OMPS generally exhibiting a negative bias, except between 32  
581 and 38 km in the tropics and southern mid-latitudes, where the bias is positive. Between 20 and 45 km in the tropics  
582 and southern mid-latitudes the differences between OMPS LP and MLS, and OMPS LP and SAGE III/ISS are less  
583 than  $\pm 5\%$ . Above 50 km, the agreement with MLS is still on the order of -5% or better, but differences with SAGE  
584 III/ISS and ACE-FTS start to increase with increasing altitude, which is consistent with the SAGE III/ISS and ACE-  
585 FTS validation results which show that both instruments have an increasing positive bias in the upper stratosphere.  
586 Below 20 km, larger positive biases, up to  $\sim 35\%$ , are seen in the tropical tropopause layer ( $\sim 15$  to  $20$  km) between  
587 approximately  $40^{\circ}$  S and  $40^{\circ}$  N. In the southern mid-latitudes OMPS LP agrees to within  $\sim 12\%$  between 12 and 20  
588 km when compared to ACE-FTS and sondes, but shows slightly larger differences with MLS and SAGE III/ISS below  
589 15 km. Below 20 km in the northern mid-latitudes, the biases between OMPS LP and all correlative measurements  
590 are comparable, and range from a positive bias of  $\sim 10\%$  at 18 km down to a small negative bias of  $< 5\%$  at 12 km.  
591 Almost all of the observed biases when compared to correlative satellite data fall within the reported biases and  
592 precisions of those instruments, particularly in the 20 to 45 km altitude range.

593  
594  
595  
596  
597  
598

We now have more than 12 years of OMPS LP ozone retrievals, and this allows us to evaluate both the seasonal cycle and the long-term stability of the data, which we have done by comparing to satellite and ozonesonde data. We find that OMPS version 2.6 ozone exhibits the same seasonal cycle as compared to all correlative measurement sources and our analysis shows that there is no significant seasonal bias in the OMPS LP.

599  
600  
601  
602  
603  
604  
605  
606  
607  
608  
609  
610

To evaluate the long term stability of OMPS LP ozone we calculate the drifts between OMPS LP and correlative data sources using deseasonalized monthly mean differences, see table 1. We find mean relative drifts at all latitude bands of less than  $\pm 2\%$ /decade between 25 and 55 km, with larger drifts of up to  $\pm 5\%$ /decade below 20 km, these represent an improvement over OMPS LP version 2.5 ozone. However, there is a spread in these drifts between correlative sources that often straddles the zero line. In order to confidently detect long-term ozone trends in the stratosphere, a threshold stability requirement of 3% per decade for ozone stratospheric profiles has been set by the World Meteorological Organisation (WMO 2022). We therefore conclude that there is no significant systematic drift in OMPS LP version 2.6 ozone for the period 2012 to 2024 and that OMPS LP data meets current WMO requirements for long-term stratospheric ozone trend studies. Whilst relative drifts calculated over shorter time periods can be larger, as demonstrated here for the period 2017-2024, analysis of ozone difference time series does not show any clear, consistent drifts in OMPS LP ozone over the entire record.

611  
612  
613  
614  
615  
616  
617  
618  
619  
620  
621  
622  
623  
624  
625  
626  
627  
628  
629  
630  
631  
632

Currently the best source of correlative data with which to evaluate OMPS LP ozone profile retrievals is Aura MLS as it is able to provide high vertical resolution profiles with dense geospatial sampling. However, MLS is scheduled to be decommissioned within the next year, and so other sources of data must be found. In this paper, in addition to MLS, we have used solar occultation satellite instrument data from ACE-FTS and SAGE III/ISS to evaluate OMPS LP ozone profiles. Although solar occultation instruments are able to provide high vertical resolution ozone profiles the number of profiles observed per day by these instruments is very small compared to OMPS LP, and their spatial coverage is very limited and varies seasonally. The limited number of observations and lack of spatial coverage means that in order to make meaningful global comparisons one must average over wide latitude bands and longer time scales. It also means that longer time periods are needed in order to calculate reliable drifts. Ozonesondes and lidar observations are able to provide high vertical resolution ozone profiles with which to evaluate OMPS LP profiles, however they lack the geospatial coverage afforded by a satellite instrument such as MLS. Together, independent solar occultation and ozonesonde measurements can be used to continuously monitor for potential drifts in OMPS LP, while LP provides the near global coverage necessary to ensure geographically representative trends. Finally, the OMPS NP series of instruments, which is able to provide full global coverage coincident with OMPS LP, but with limited vertical resolution, offers a source of data with which to evaluate OMPS LP ozone profiles, and there will always be an OMPS NP instrument on the same satellite platform as all future OMPS LP instruments. Therefore, in the future when MLS data is no longer available, a combination of ozonesondes, lidars and OMPS NPs will be needed in order to globally evaluate OMPS LP ozone profiles, with OMPS NP providing the global coverage and ozonesondes and lidars providing the high vertical resolution information needed to interpret any vertical structure seen in the OMPS LP/NP comparisons. There will also be some overlap between successive OMPS LP instruments which we can exploit in order to cross-calibrate/validate them, this will enable us to determine any bias offsets between them.

633  
634  
635  
636  
637  
638  
639  
640  
641  
642  
643  
644  
645  
646  
647  
648

| Altitude (km) | 60°S to 30°S           |                      | 30°S to 30°N          |                      | 30°N to 60°N           |                      |
|---------------|------------------------|----------------------|-----------------------|----------------------|------------------------|----------------------|
|               | Bias (%)               | Drift (%/decade)     | Bias (%)              | Drift (%/decade)     | Bias (%)               | Drift (%/decade)     |
| 15.5          | -5.84 ( $\pm 2.84$ )   | -4.74 ( $\pm 0.89$ ) | -                     | -                    | 3.34 ( $\pm 0.28$ )    | -3.50 ( $\pm 0.62$ ) |
| 20.5          | 4.32 ( $\pm 1.08$ )    | 1.87 ( $\pm 3.02$ )  | 2.32 ( $\pm 3.88$ )   | 1.14 ( $\pm 2.57$ )  | 4.14 ( $\pm 0.07$ )    | 3.44 ( $\pm 1.07$ )  |
| 25.5          | -2.31 ( $\pm 1.81$ )   | 0.44 ( $\pm 1.48$ )  | -0.86 ( $\pm 0.94$ )  | -0.40 ( $\pm 2.15$ ) | -8.15 ( $\pm 1.66$ )   | 0.93 ( $\pm 0.17$ )  |
| 30.5          | 0.65 ( $\pm 9.54$ )    | -2.38 ( $\pm 0.47$ ) | -3.90 ( $\pm 6.14$ )  | -1.41 ( $\pm 0.08$ ) | -5.29 ( $\pm 6.24$ )   | -0.54 ( $\pm 0.69$ ) |
| 35.5          | 2.61 ( $\pm 0.50$ )    | -0.22 ( $\pm 0.59$ ) | 2.58 ( $\pm 0.38$ )   | 0.91 ( $\pm 0.19$ )  | -0.43 ( $\pm 0.58$ )   | 1.24 ( $\pm 1.55$ )  |
| 40.5          | -0.21 ( $\pm 1.29$ )   | -1.75 ( $\pm 1.24$ ) | -0.35 ( $\pm 1.29$ )  | -0.22 ( $\pm 0.55$ ) | -2.02 ( $\pm 1.79$ )   | -1.06 ( $\pm 1.37$ ) |
| 45.5          | -4.57 ( $\pm 0.33$ )   | -2.12 ( $\pm 3.30$ ) | -4.07 ( $\pm 0.11$ )  | 0.22 ( $\pm 1.50$ )  | -6.76 ( $\pm 0.32$ )   | 0.54 ( $\pm 2.24$ )  |
| 50.5          | -6.48 ( $\pm 0.78$ )   | -2.11 ( $\pm 1.44$ ) | -6.61 ( $\pm 0.71$ )  | -1.16 ( $\pm 0.25$ ) | -8.41 ( $\pm 0.86$ )   | 0.11 ( $\pm 2.84$ )  |
| 55.5          | -10.59 ( $\pm 25.79$ ) | -1.21 ( $\pm 2.26$ ) | -9.43 ( $\pm 15.23$ ) | -2.32 ( $\pm 0.12$ ) | -13.18 ( $\pm 21.80$ ) | 1.59 ( $\pm 4.49$ )  |

649  
650 **Table 1: Mean biases and relative drifts at 9 specified altitudes for 3 wide latitude bands. The mean biases were derived by**  
651 **using the relative biases between OMPS LP and all high vertical resolution observations (Ozonesondes, MLS, ACE-FTS**  
652 **and SAGE III/ISS) for the period April 2012 to April 2024 (2017-2024 for SAGE III/ISS). The mean drifts were calculated**  
653 **using only the relative drifts for which there were data for the whole OMPS LP time period (2012-2024) and therefore**  
654 **exclude SAGE III/ISS data. The numbers in brackets represent the unbiased estimator of the standard error of the mean**  
655 **as described in equation 5.1 in the 2018 LOTUS report (SPARC/IO3C/GAW, 2019).**

## 657 Data Availability

658 SNPP OMPS LP version 2.6 ozone profile data are available at the NASA Goddard Earth Sciences Data and  
659 Information Services Center (GES DISC): <https://disc.gsfc.nasa.gov/>

660 MLS data are available at the NASA Goddard Earth Sciences Data and Information Services Center (GES DISC):  
661 <https://disc.gsfc.nasa.gov/>

662 ACE-FTS data are available via the ACE/SCISAT database: <https://databace.scisat.ca/>

663 SAGE III/ISS data are available at the NASA Langley Atmospheric Science Data Center (ASDC):  
664 <https://asdc.larc.nasa.gov/>

665 Ozone sonde data are available at the NASA Goddard Atmospheric composition Validation Data Center (AVDC):  
666 <https://avdc.gsfc.nasa.gov/>

667 Mauna Loa lidar data are available via the Network for the Detection of Atmospheric Composition Change (NDACC):  
668 <https://ndacc.larc.nasa.gov/>

669 OMPS NP data are available at the NASA Goddard Earth Sciences Data and Information Services Center (GES DISC):  
670 <https://disc.gsfc.nasa.gov/>

## 679 Author contribution

681 NK directed the work, NR and NK devised the comparison methodology, NR carried out the work and NK and NR  
682 analyzed the results. SD and YJ performed the comparisons between OMPS LP and the MLO lidar station. NR  
683 prepared the manuscript with contributions from all co-authors.

684 **Competing interests**

685  
686 Some of the authors are members of the editorial board of Atmospheric Measurement Techniques.

687 **Acknowledgements**

688  
689 This research is supported by the GESTAR II Cooperative Agreement with NASA Goddard Space Flight Center

690 **References**

691  
692 Benito-Barca, S., Abalos, M., Calvo, N., Garny, H., Birner, T., Abraham, N. L., et al. (2025). Recent lower  
693 stratospheric ozone trends in CCMCI-2022 models: Role of natural variability and transport. *Journal of Geophysical*  
694 *Research: Atmospheres*, 130, e2024JD042412. <https://doi.org/10.1029/2024JD042412>

695 Bernath, P. F. (2017). The Atmospheric Chemistry Experiment (ACE). *Journal of Quantitative Spectroscopy and*  
696 *Radiative Transfer*, 186, 3–16. <https://doi.org/10.1016/j.jqsrt.2016.04.006>

697 Bernath, P. F., McElroy, C. T., Abrams, M. C., Boone, C. D., Butler, M., Camy-Peyret, C., et al. (2005). Atmospheric  
698 Chemistry Experiment (ACE): Mission overview. *Geophysical Research Letters*, 32, L15S01.  
699 <https://doi.org/10.1029/2005GL022386>

700 Bernath, P., Boone, C., Lecours, M., Crouse, J., Steffen, J., Schmidt, M. (2025). Global Satellite-Based Atmospheric  
701 Profiles from Atmospheric Chemistry Experiment SciSat Level 2 Processed Data, v5.2, 2004–2024. Federated  
702 Research Data Repository. <https://doi.org/10.20383/103.01245>

703 Cisewski, M., Joseph Zawodny, Joseph Gasbarre, Richard Eckman, Nandkishore Topiwala, Otilia Rodriguez-  
704 Alvarez, Dianne Cheek, and Steve Hall "The Stratospheric Aerosol and Gas Experiment (SAGE III) on the  
705 International Space Station (ISS) Mission", *Proc. SPIE 9241, Sensors, Systems, and Next-Generation Satellites*  
706 *XVIII*, 924107 (11 November 2014); <https://doi.org/10.1117/12.2073131>

707 Farman, J. C., Gardiner, B. G., & Shanklin, J. D. (1985). Large losses of ozone in Antarctica reveal seasonal  
708 ClO<sub>x</sub>/NO<sub>x</sub> interaction. *Nature*, 315(6016), 207–210. <https://doi.org/10.1038/315207a0>

709 Flynn, L. E., Seftor, C. J., Larsen, J. C., & Xu, P. (2006). The ozone mapping and profiler suite. In J. J. Qu, W. Gao,  
710 M. Kafatos, R. E. Murphy, & V. V. Salomonson (Eds.), *Earth science satellite remote sensing* (pp. 279–296).  
711 Springer. [https://doi.org/10.1007/978-3-540-37293-6\\_15](https://doi.org/10.1007/978-3-540-37293-6_15)

712 Frith, S. M., Bhartia, P. K., Oman, L. D., Kramarova, N. A., McPeters, R. D., and Labow, G. J.: Model-based  
713 climatology of diurnal variability in stratospheric ozone as a data analysis tool, *Atmos. Meas. Tech.*, 13, 2733–  
714 2749, <https://doi.org/10.5194/amt-13-2733-2020>, 2020.

715 Godin-Beekmann, S., Azouz, N., Bandyopadhyay, P., et al. (2023). Updated trends of the stratospheric ozone vertical  
716 distribution in the 60° S–60° N latitude range based on the LOTUS regression model. *Atmospheric Chemistry and*  
717 *Physics*, 23(9), 4871–4899. <https://doi.org/10.5194/acp-22-11657-2022>

718 Kramarova, N. A., Nash, E. R., Newman, P. A., Bhartia, P. K., McPeters, R. D., Rault, D. F., et al. (2014). Measuring  
719 the Antarctic ozone hole with the new ozone mapping and profiler suite (OMPS). *Atmospheric Chemistry and*  
720 *Physics*, 14(5), 2353–2361. <https://doi.org/10.5194/acp-14-2353-2014>

721 Kramarova, N. A., Bhartia, P. K., Jaross, G., Moy, L., Xu, P., Chen, Z., et al. (2018). Validation of ozone profile  
722 retrievals derived from the OMPS LP version 2.5 algorithm against correlative satellite measurements. *Atmospheric*  
723 *Measurement Techniques*, 11(5), 2837–2861. <https://doi.org/10.5194/amt-11-2837-2018>

724 Kramarova, N. A. (2023). OMPS-NPP L2 LP ozone (O<sub>3</sub>) vertical profile swath daily center slit V2.6 [Dataset]. *NASA*  
725 *Goddard Earth Sciences Data and Information Services Center*. <https://doi.org/10.5067/8MO7DEDYTBH7>

726 Kramarova, N. A., & DeLand, M. (2023). README document for the Suomi-NPP OMPS LP L2 O<sub>3</sub> daily product  
727 (version 2.6) (p. 36). *Goddard Earth Sciences Data and Information Services Center (GES DISC)*. Retrieved from  
728 [https://disc.gsfc.nasa.gov/datasets/OMPS\\_NPP\\_LP\\_L2\\_O3\\_DAILY\\_2.6/summary?keywords=OMPS](https://disc.gsfc.nasa.gov/datasets/OMPS_NPP_LP_L2_O3_DAILY_2.6/summary?keywords=OMPS)

729 Kramarova, N. A., Xu, P., Mok, J., Bhartia, P. K., Jaross, G., Moy, L., et al. (2024). Decade-long ozone profile record  
 730 from Suomi NPP OMPS Limb Profiler: Assessment of version 2.6 data. *Earth and Space Science*, 11,  
 731 e2024EA003707. <https://doi.org/10.1029/2024EA003707>

732 Leblanc, T., and I. Stuart McDermid. (2000). Stratospheric ozone climatology from lidar measurements at Table  
 733 Mountain (34.4°N, 117.7°W) and Mauna Loa (19.5°N, 155.6°W). *Journal of Geophysical Research*, 105, 14613-  
 734 14623. <https://doi.org/10.1029/2000JD900030>

735 Livesey, N. J., Read, W. G., Wagner, P. A., Froidevaux, L., Santee, M. L., Schwartz, M. J., et al. (2022). *Version 5.0x*  
 736 *Level 2 and 3 data quality and description document* (Tech. Rep. No. JPL D-105336 Rev. B). Jet Propulsion  
 737 Laboratory. Downloaded from [https://mls.jpl.nasa.gov/data/v5-0\\_data\\_quality\\_document.pdf](https://mls.jpl.nasa.gov/data/v5-0_data_quality_document.pdf)

738 McPeters, R., Frith, S., Kramarova, N., Ziemke, J., and Labow, G.: Trend quality ozone from NPP OMPS: the version  
 739 2 processing, *Atmos. Meas. Tech.*, 12, 977–985, <https://doi.org/10.5194/amt-12-977-2019>, 2019.

740 Rault, D. F., & Loughman, R. P. (2013). The OMPS limb profiler environmental data record algorithm theoretical  
 741 basis document and expected performance. *IEEE Transactions on Geoscience and Remote Sensing*, 51(5), 2505–  
 742 2527. <https://doi.org/10.1109/TGRS.2012.2213093>

743 SAGE III/ISS Data Products User's Guide, Version 6.0, 2025, [https://asdc.larc.nasa.gov/documents/sageiii-iss\\_guide/data\\_product\\_users\\_guide\\_6.0.pdf](https://asdc.larc.nasa.gov/documents/sageiii-iss_guide/data_product_users_guide_6.0.pdf)

744 Salawitch, R. J., J. B. Smith, H. Selkirk, et al. (2025), The Imminent Data Desert: The Future of Stratospheric  
 745 Monitoring in a Changing Climate, *Bulletin of the American Meteorological Society*,  
 746 <https://doi.org/10.1175/BAMS-D-23-0281.1>

747 Sheese, Patrick; Walker, Kaley, 2023, Data Quality Flags for ACE-FTS Level 2 Version 5.2 Data Set, *Borealis*,  
 748 V16. <https://doi.org/10.5683/SP3/NAYNFE>

749 SPARC/IO3C/GAW, 2019: SPARC/IO3C/GAW Report on Long-term Ozone Trends and Uncertainties in the  
 750 Stratosphere. I. Petropavlovskikh, S. Godin-Beekmann, D. Hubert, R. Damadeo, B. Hassler, V. Sofieva (Eds.),  
 751 SPARC Report No. 9, GAW Report No. 241, WCRP-17/2018, doi: 10.17874/f899e57a20b, available at [www.sparc-climate.org/publications/sparc-reports](http://www.sparc-climate.org/publications/sparc-reports)

752 Stauffer, R. M., Thompson, A. M., Kollonige, D. E., Tarasick, D. W., van Malderen, R., Smit, H. G. J., Vömel, H.,  
 753 Morris, G. A., Johnson, B. J., Cullis, P. D., Stübi, R., Davis, J., and Yan, M. M. (2022). An examination of the  
 754 recent stability of ozonesonde global network data, *Earth and Space Science*, 9, e2022EA002459,  
 755 <https://doi.org/10.1029/2022EA002459>, 2022

756 Wang, H. J. R., Damadeo, R., Flittner, D., Kramarova, N., Taha, G., Davis, S., et al. (2020). Validation of SAGE  
 757 III/ISS solar occultation ozone products with correlative satellite and ground based measurements. *Journal of*  
 758 *Geophysical Research: Atmospheres*, 125, e2020JD032430. <https://doi.org/10.1029/2020JD032430>

759 WMO (World Meteorological Organization). (2022). Scientific assessment of ozone depletion: 2022 (GAW report  
 760 No. 278) (p. 509). WMO. Downloaded from <https://ozone.unep.org/science/assessment/sap>

761 World Meteorological Organisation: GCOS-22: The 2022 GCOS ECVs Requirements, WMO GCOS-245, World  
 762 Meteorological Organisation, <https://library.wmo.int/idurl/4/58111> (last access: 1 December 2025), 2022.